

Conodont-based event stratigraphy of the Early–Middle Frasnian transition on the South Polish carbonate shelf

AGNIESZKA PISARZOWSKA, MAŁGORZATA SOBTEL, and GRZEGORZ RACKI



Pisarzowska, A., Sobtel, M., and Racki, G. 2006. Conodont-based event stratigraphy of the Early–Middle Frasnian transition on the South Polish carbonate shelf. *Acta Palaeontologica Polonica* 51 (4): 609–646.

Early to Middle Frasnian (E–MF) epicontinental sequences are investigated in five representative localities of the Holy Cross Mountains and Cracow region, with emphasis on conodont biostratigraphy, to evaluate the regional stratigraphic and biotic context of a major biogeochemical perturbation in global carbon cycling. Conodont associations from the *Palmatolepis transitans* to *Palmatolepis punctata* Zone boundary beds are dominated by the shallow-water polygnathid and ancyrodellid fauna in the South Polish epicontinental successions, and first appearances of index palmatolepid species are delayed due to facies control of pelagic environments during intermittent drowning of the carbonate shelf. Thus, identification of the zonal boundary is based mainly on species of *Ancyrodella*, and five distinctive ancyrodellid levels in the succession across the E–MF interval enable refined correlation of the sections studied, especially when paired with chemostratigraphic proxies. Prominent conodont biofacies shifts coincided with eustatic deepening, which is correlated with the Timan, Middlesex, and early Rhinestreet events, respectively. Trends in the conodont dynamics, mortality and diversity, partly replicated by the benthic biota (especially shelly faunas and crinoids), indicate that the faunal turnovers correlate also with the main $\delta^{13}\text{C}$ excursions and related changes in trophic conditions. The E–MF transitional interval, marked by short-term sea-level fluctuations, is distinguished by a change from relatively diversified biofacies to more homogenous, mostly impoverished faunas. The latter change is a biotic response to the beginning of a prolonged (ca. 0.5 Ma) positive $\delta^{13}\text{C}$ anomaly, probably paired with unsteady eutrophic and partly anoxic regimes. The late *Pa. punctata* Zone negative carbon isotope anomaly is synchronous with the second large-scale pelagic biofacies remodelling, including mesotaxid extinction. A stabilization of the carbon cycle and its return to normal background values at the start of the Early *Palmatolepis hassi* Zone coincide with conodont biofacies diversification and recovery of reef-related biofacies. With the exception of collapsed, endemic Kadzielnia-type mud-mound biota and a moderate biodiversity depletion due to overall ecosystem stagnation, no significant extinction events can be demonstrated, even if the large-scale changes in carbon cycling during the E–MF timespan are of higher-amplitude than the celebrated carbon isotopic anomalies related to the Frasnian–Famennian mass extinction. Thus, this regional succession in detail confirms that the large-scale *punctata* Isotopic Event (= *Pa. punctata* Event) is correlated neither with catastrophic environmental nor radical biotic changes.

Key words: Biostratigraphy, carbon isotopes, paleoecology, benthos, pelagic biota, Devonian, Frasnian, Poland.

Agnieszka Pisarzowska [apiechot@wnoz.us.edu.pl] and Małgorzata Sobtel [penczek@wnoz.us.edu.pl], Wydział Nauk o Ziemi, Uniwersytet Śląski, ul. Będzińska 60, PL-41-200 Sosnowiec, Poland;

Grzegorz Racki [racki@us.edu.pl], Wydział Nauk o Ziemi, Uniwersytet Śląski, ul. Będzińska 60, PL-41-200 Sosnowiec, Poland; present address: Instytut Paleobiologii PAN, ul. Twarda 51/55, PL-00-818 Warszawa, Poland.

Introduction

The Early–Middle Frasnian (E–MF) boundary beds, corresponding to the *Palmatolepis transitans*–*Palmatolepis punctata* conodont zonal boundary (as formally recommended by the Subcommission on Devonian Stratigraphy, SDS; Becker and House 1998; Ziegler and Sandberg 2001), are well exposed in the South Polish–Moravian bank-to-reef successions, exemplified by the Holy Cross Mountains (Figs. 1–3; see summary in Racki 1993b). Although well studied in terms of its facies, paleontology and stratigraphy (e.g., Szulczeński 1971; Wrzołek 1988; Racki 1993a, b; Racki and Bultynck 1993; Baliński 1995; Dzik 2002; Krawczyński 2002), this Late Devonian interval remains relatively poorly known, especially from a geochemical viewpoint.

The epicontinental sequences are investigated in five representative localities of the Holy Cross Mountains (with reference section at Wietrzna, Kielce; Figs. 1B, 2, and 4B, C) and Cracow region (Fig. 1A), with emphasis on conodont biostratigraphy, to evaluate the regional stratigraphic, facies and biotic context of a recently recognized major biogeochemical perturbation in global carbon cycling across the E–MF transition (see Racki 2005). In fact, the integrative event-stratigraphic study herein was inspired by results of a previous Belgian-Polish geochemical study presented in Racki et al. (2004) and Yans et al. (in press). The aim of this article is to outline the shelf ecosystem evolution recorded in the southeastern Lauroussian successions, as a summary of an international project “Ecosystem aspects of major carbon isotope anomaly in the Lower–Middle Frasnian transition” (grant 3 P04D 040 22 to

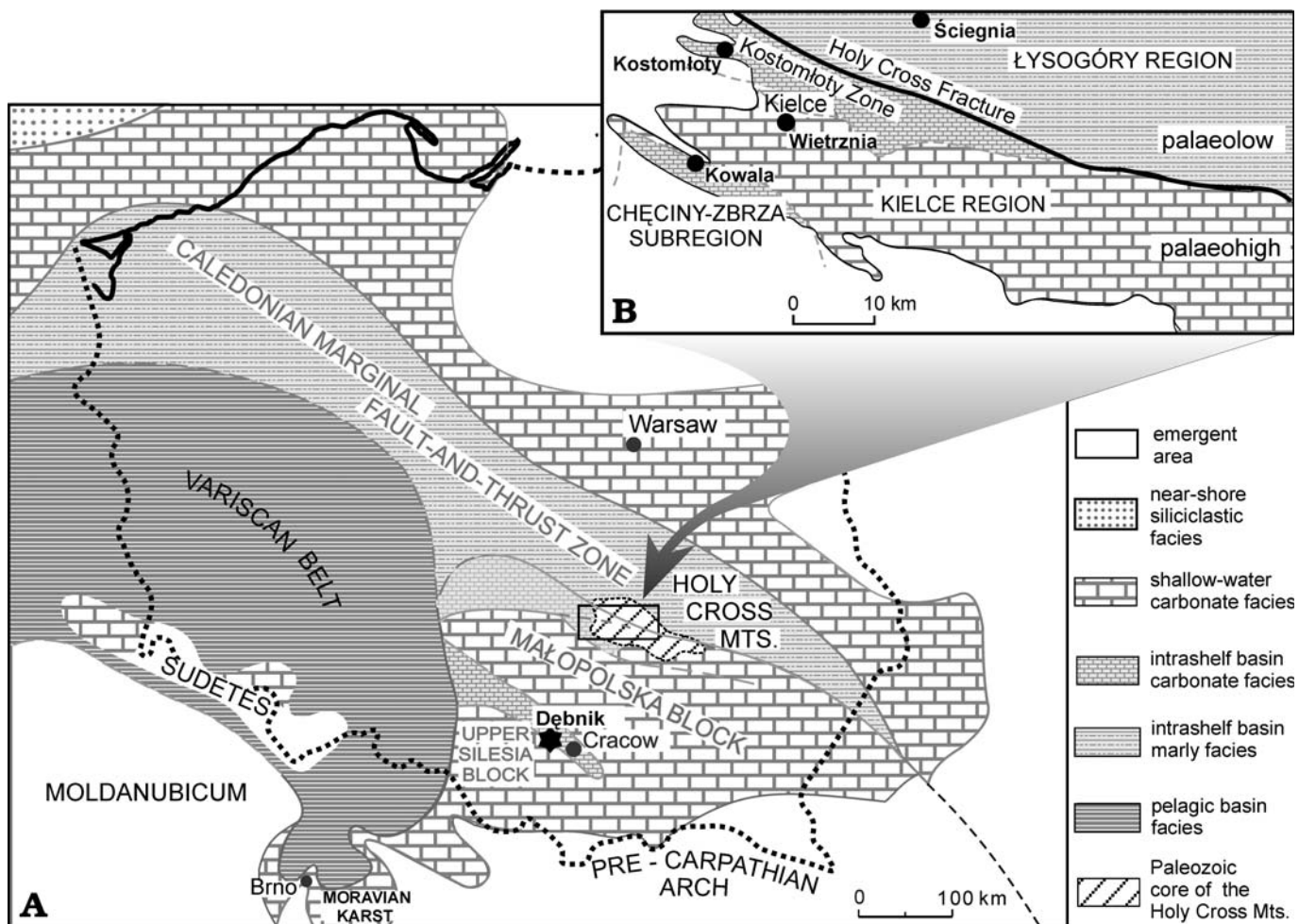


Fig. 1. Location of studied localities within the paleogeographic and structural framework of the Givetian to Frasnian in Poland (A; after Racki 1993b: fig. 1), and Holy Cross Mountains (B; based on Racki 1993b: fig. 2).

G. Racki), supported by the Committee for Scientific Research in Poland. Carbon isotopic data, and other geochemical aspects will be described in detail in papers published elsewhere by A. Pisarzowska and other members of Racki's research group.

A. Pisarzowska is responsible for regional litho- and chemostratigraphic data, M. Sobstel for conodont biostratigraphy, other discussions are joint, but mostly led by G. Racki.

Institutional abbreviation.—GIUS, Department of Paleontology and Biostratigraphy of the University of Silesia, Sosnowiec, Poland.

Other abbreviations.—E–MF, Early–Middle Frasnian; MN, Montagne Noire conodont zones of Klapper (1988); MS, magnetosusceptibility; SDS, Subcommission on Devonian Stratigraphy.

Regional setting

Devonian strata of the Holy Cross Mountains belong to an elongated belt between the southwestern margin of the East

European Craton and Variscan Deformation Front (Fig. 1A), delineating the currently debated extent of the Wielkopolska and Silesian-Moravian (-Precarpathian?) Variscides, as summarized by Dadlez et al. (1994). According to these authors, the Devonian overlap sequence developed both over a fragment of the Caledonian marginal fold-and-thrust zone and over two possible terranes comprising the proximal Małopolska Block and exotic(?) Upper Silesia Block (for a more recent interpretation, see Dadlez 2001 and Schätz et al. 2006).

The shelf, up to 600 km in width, formed the Polish fragment of a pericratonic basin stretching from Western Europe to Ukraine along the periphery of the "Old Red Sandstone Continent" (Laurussia). The southern part of the basin, extending to the Moravian Karst and Sub-Carpathian area (Fig. 1A), is best known from numerous outcrops in the Holy Cross Mountains and Silesia-Cracow area, as well as from intensive borehole data. Two distinct paleogeographic-tectonic regions of the Holy Cross area (the Kielce paleohigh and Łysogóry paleolow; Fig. 1B) offer an opportunity to compare the event record across the Early–Middle Frasnian boundary in several sedimentary regimes (Fig. 3). The separating Holy Cross Fault zone is the result of the interaction of evolving transtensional

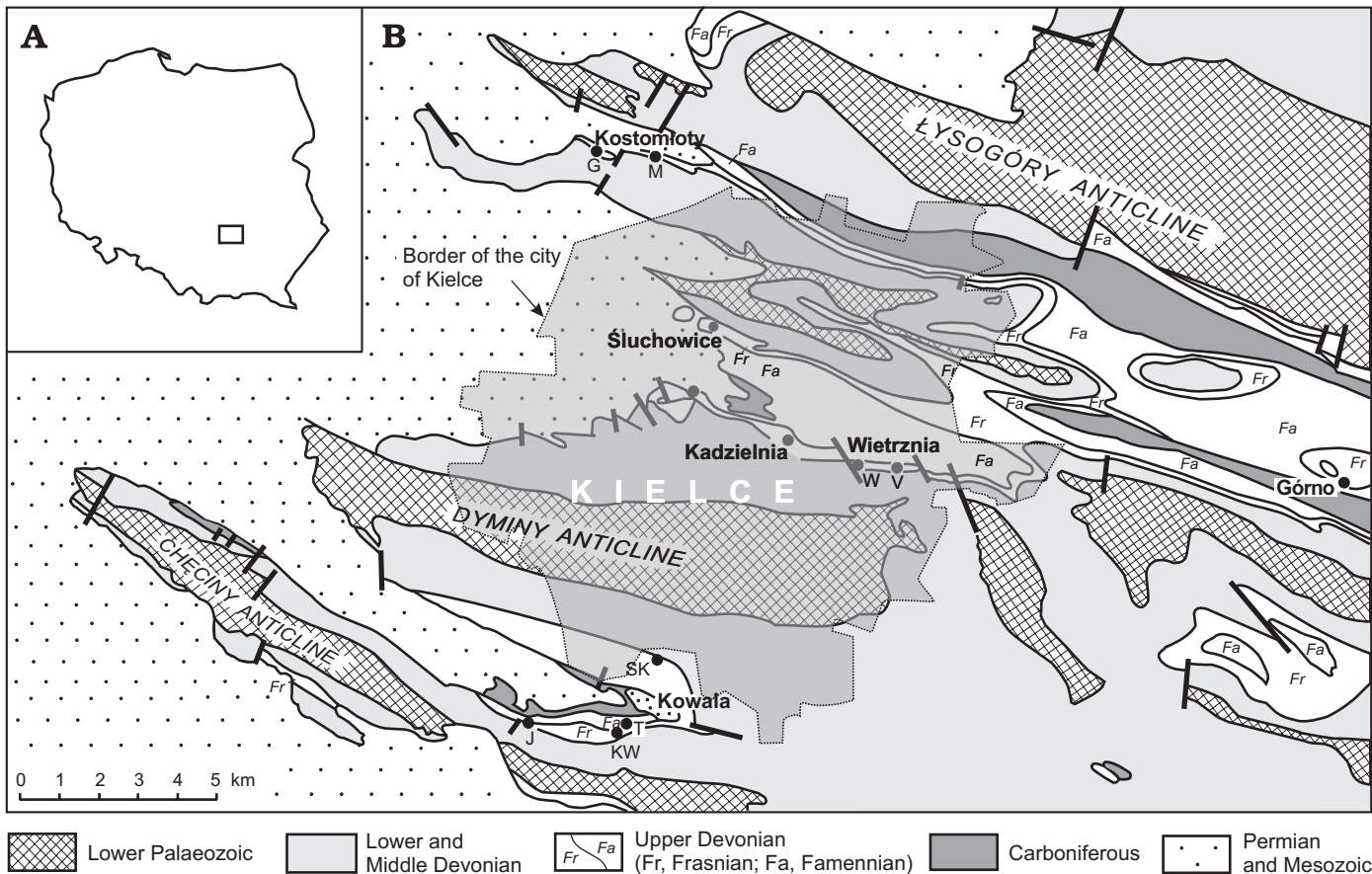


Fig. 2. Location map of studied Early to Middle Frasnian exposures in Poland (A) and Holy Cross Mountains (B; based on Szulczewski 1971: fig. 1). Abbreviations: G, Małe Górkı quarry; J, Jaźwica quarry; KW, Kowala railroad cut; M, Mogiłki quarry; SK, unused Sitkówka-Kowala; T, active Kowala quarry; V, Wietrzna II quarry; W, unused Wietrzna I quarry (see Fig. 6).

and transpressional regimes during the Variscan diastrophic cycle, recorded finally in the flower-like structure of the zone (Lamarche et al. 2003). This structural framework controlled Early Devonian continental and marginal marine clastics, obviously related to post-Caledonian erosional relief. The sub-symmetric facies plan is shown by the central location of the Frasnian Dyminy Reef (Figs. 1B, 3; see Szulczewski 1995 for summary), which is surrounded by two intrashelf basins: the Chęciny-Zbrza to the south and the Łysogóry-Kostomłoty to the north. The key position is occupied by the Dyminy Reef that developed over the northern peripheral zone of the Kielce carbonate platform at the site of the Caledonian rise (Narkiewicz 1988; Racki 1993b). The Late Devonian epicontinental succession indicates continuous but punctuated drowning of an increasingly differentiated carbonate platform (Fig. 3), which was finally completed in the Visean (Szulczewski 1995). However, the shelf domain was influenced also by early Variscan extensional tectonics, and the resulting normal fault system exerted essential structural control over later Variscan tectonic inversion and Alpine deformations (Lamarche et al. 2003).

The southern closure of the shelf was formed mostly by the poorly known Sub-Carpathian Arch (Narkiewicz 1988, 1996). A facies transect exhibits gradual shallowing south-

twards toward this stable, elevated area, which was occupied by a low-angle attached carbonate platform (Narkiewicz 1988: fig. 4), and the well-studied Zawiercie-Dębnik cross-section is situated at the northeastern periphery of the stable Upper Silesian Block, in the zone of a Caledonian suture (Fig. 1A; see Dadlez et al. 1994). The southern Frasnian sections are well documented at Dębnik near Kraków (Baliński 1979; Narkiewicz and Racki 1984).

The Early–Middle Frasnian boundary beds are more or less confidently dated with conodonts in most Holy Cross Mountains sections, as well as within other Polish epicontinental successions (e.g., Szulczewski 1971; Narkiewicz and Racki 1984; Racki and Bultynck 1993; Sobstel 2003). Among accessible exposures (for details of locations see “Register of localities” in Racki 1993b), grouped mostly in the western part of the Holy Cross Mountains (Figs. 2, 3), only the most representative sections are analysed bed-by-bed, and their lithology and conodont content are presented below (see Figs. 4–12). The continuous sedimentary successions include a record of global and regional geochemical and biotic events in different facies ranging from intrashelf basin to near-reef (foreslope) settings, and the Wietrzna downslope section was selected to provide the most comprehensive data from a deeper water setting. The present high-resolution biostratigraphical study fo-

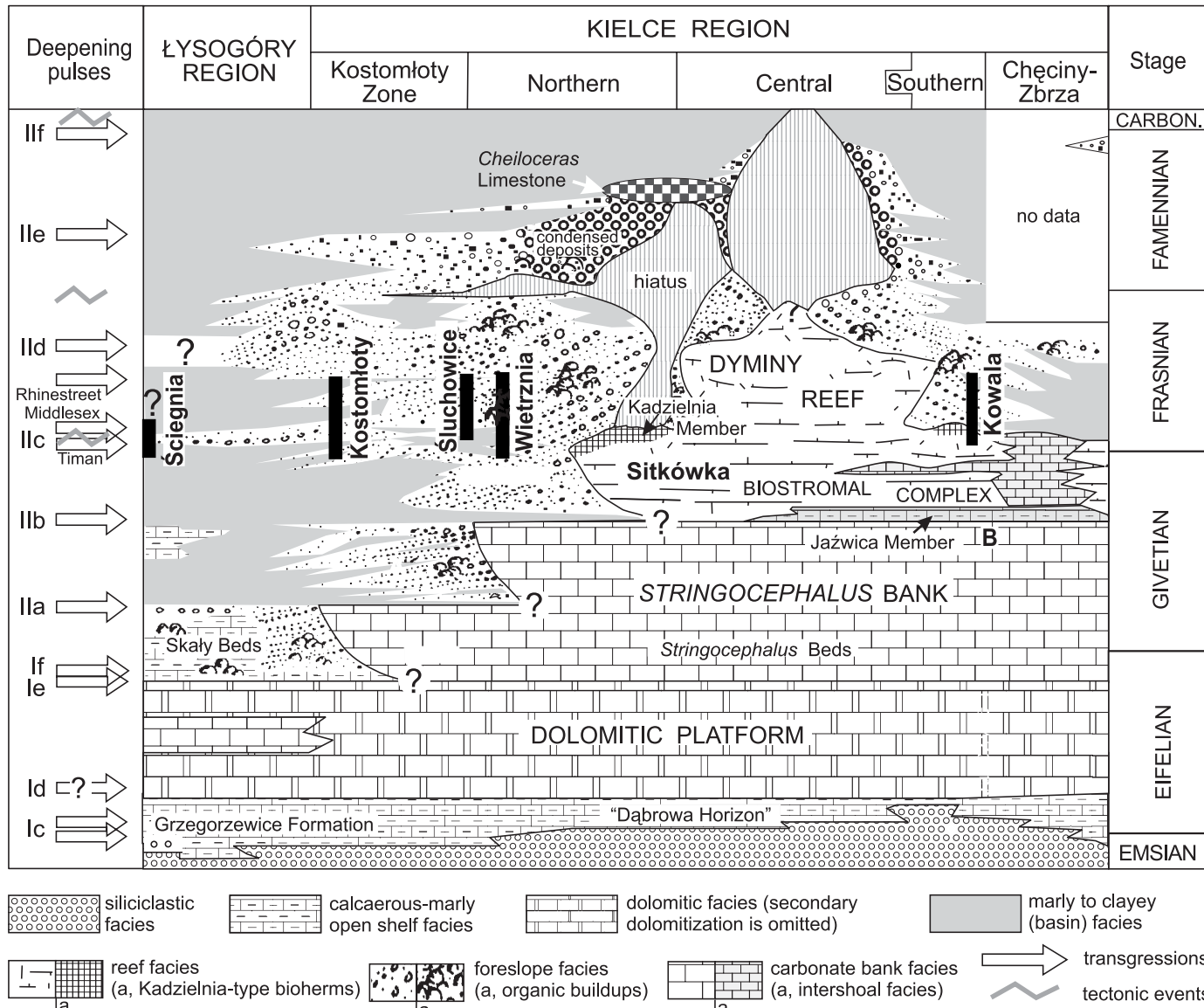


Fig. 3. Location of Early to Middle Frasnian sections studied (Fig. 2) against developmental stages of the Middle to Late Devonian bank-to-reef complex of the Holy Cross Mountains; stratigraphic-facies cross-section (after Racki 1993b: fig. 3, changed) is shown to emphasise eustatic rhythmic control of the depositional pattern; Ic-IIf, transgressive-regressive cycles modified from Johnson et al. (1985), and Timan, Middlesex, and Rhinestreet deepening pulses summarized in House (2002) and House and Gradstein (2004).

cused on the precise conodont-based recognition of the E-MF boundary in the logged sections and their accurate bio- and chemostratigraphic correlations as a prerequisite to the event-stratigraphic interpretations of the eventful Frasnian interval.

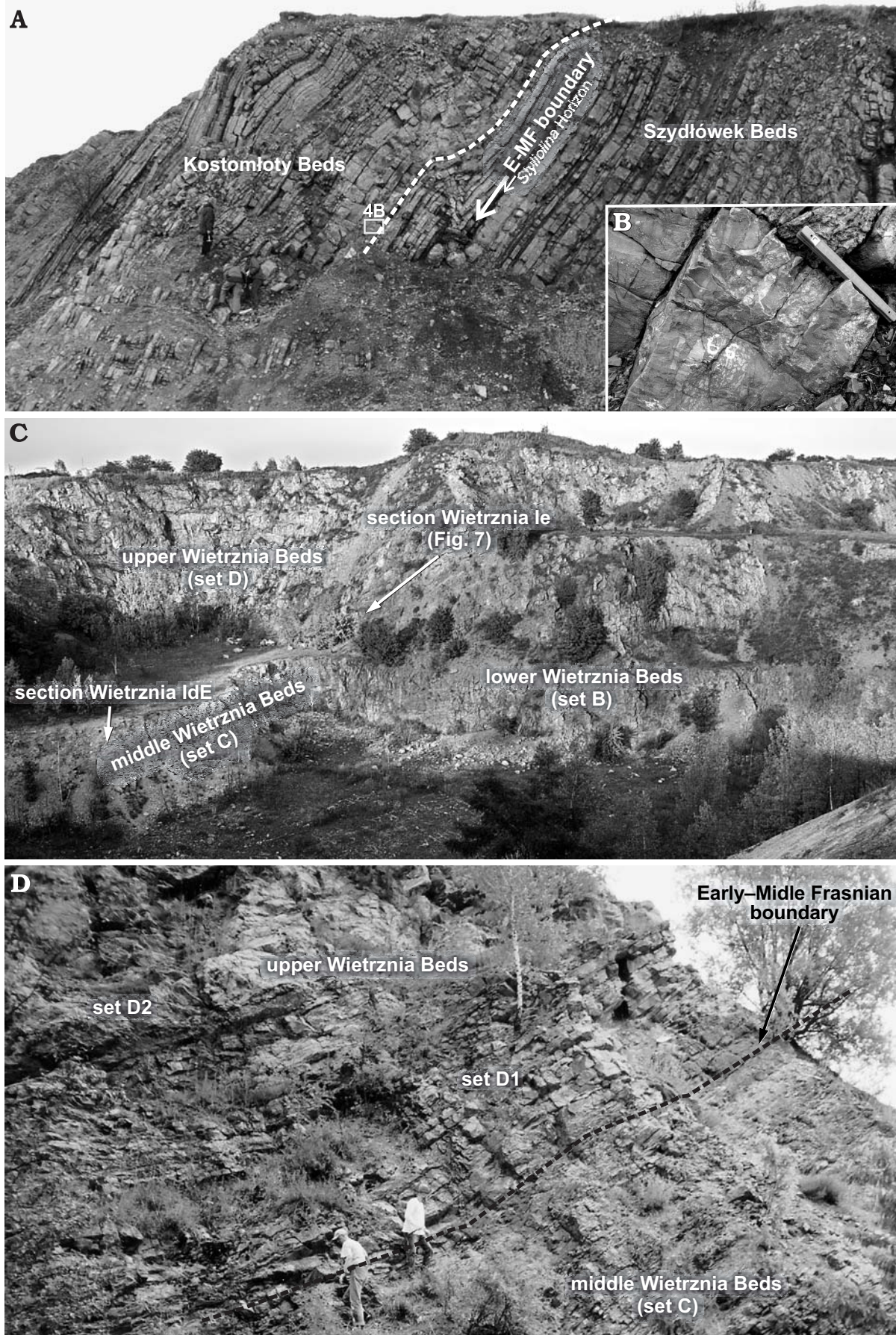
Wietrzna reference section

Three sections, Wietrzna Id-W (WId-W), Wietrzna Id-E (WId-E) and Wietrzna Ie (WIE), designated after Szulczewski (1971), Racki et al. (1993) and Makowska (2001), are

studied on the Wietrzna Hill in a large, inactive quarry (Fig. 6). The locality is situated in the eastern Kadzielnia Chain, in the southern part of Kielce, within the southern limb of the Kielce Syncline. The above sections are located in the northern part of the Wietrzna I quarry, and WId-W section corresponds to the most western part, and WIE to the eastern wall (Figs. 4C, D and 6). A distinct NNW-SSE oriented fault separates the WId and WIE outcrops; the latter one was selected for the most comprehensive study (Fig. 7).

In exposed Frasnian limestones, Szulczewski (1971) has distinguished five units or sets (A through E). Our study con-

Fig. 4. Field photos of outcrops under study Kostomłoty-Mogilki (A; see Figs. 2, 10), with close-up of intraclastic conglomerate in the basal Kostomłoty Beds (B; scale bar 20 cm), and Wietrzna I (C, D; see Figs. 2, 6, 7).



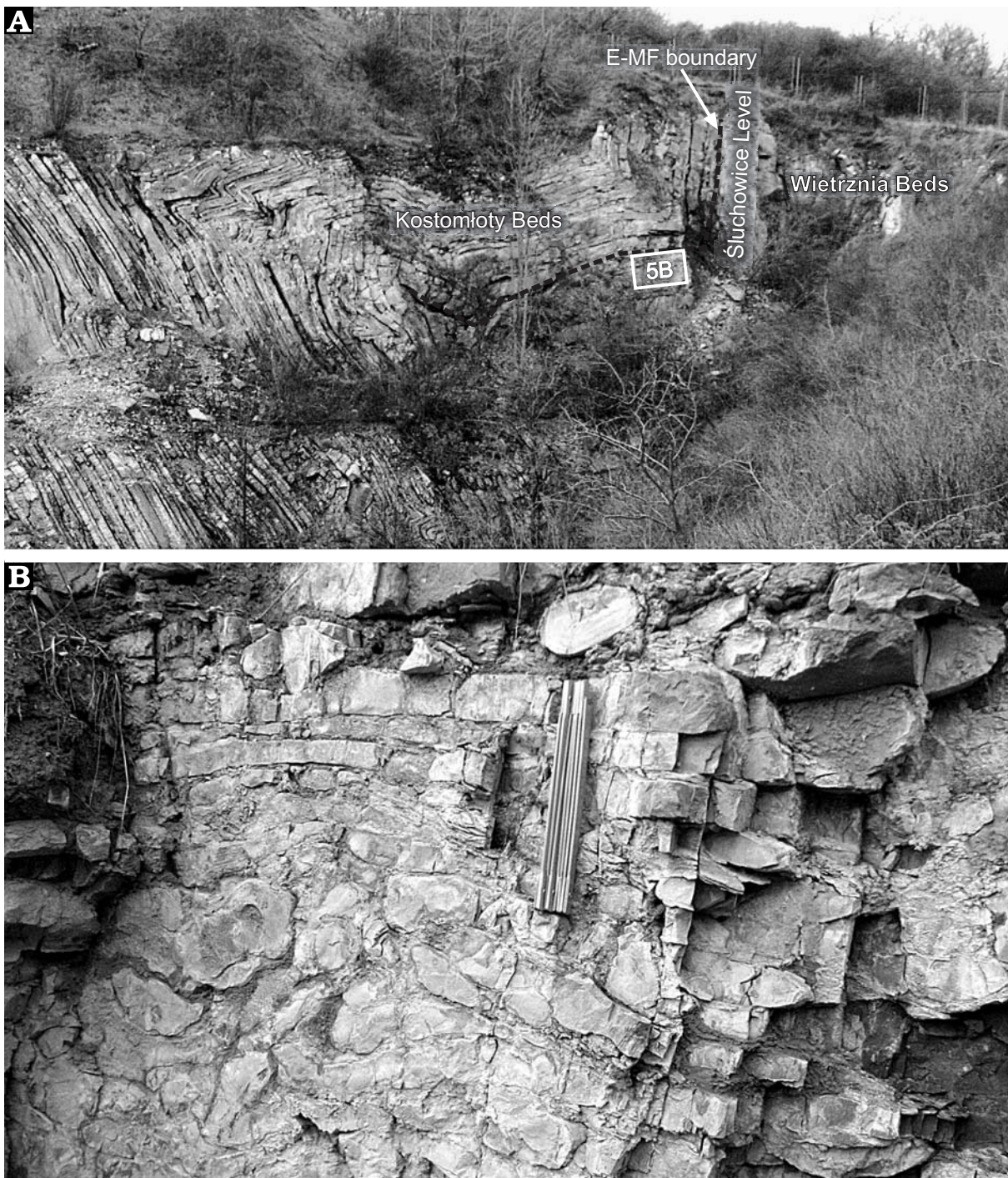


Fig. 5. Field photo of studied eastern quarry at Śluchowice (A; see Figs. 2, 9), with close-up of very-thin bedded Śluchowice Marly Level, showing initial slump folds and flat pebbles (B; scale bar 20 cm; compare with Szulczeński 1968: fig. 2).

cerned only the uppermost part of set B, the entire set C and the lower part of set D (Figs. 7, 8), i.e., the middle Wietrznią Beds (= *Phlogiderhynchus* Marly Level and surrounding strata *sensu* Racki 1993b). The topmost part of set B is visible in the WId-W and WId-E outcrops. This unit includes thick-bedded to almost massive light-coloured biorudites, sporadically interbedded with micrite and shale. Rich broken and redeposited fossils include tabular and rugose corals,

stromatoporoids, brachiopods and crinoids debris (see also Szulczeński 1971; Racki et al. 1993).

The set C exhibits a distinct lateral variation traced over a distance of ca. 100 m in the studied outcrop. In the proximal WId-W section, set C comprises thin beds of knobby and/or wavy-bedded bituminous, often laminated micrites intercalated with marly shales (Fig. 8); autochthonous brachiopod nests and bioturbation fabrics are distinctive features of some

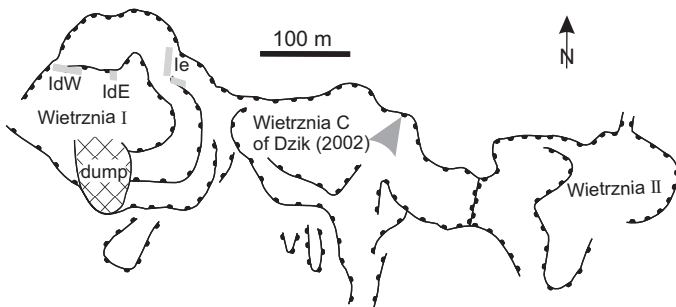


Fig. 6. Location sketch of Wietrzna quarry sections at Kielce (see Figs. 2, 7, 8).

layers (Racki et al. 1993; Vierek in press), as well as infrequent styliolinids and other calcareous microfossils (Skwarek 1990). Thicker layers of calcirudites with intraclastic and skeletal interbeds (maximally 0.75 m; layer 37), with erosional bottom surfaces, including flat-pebble conglomerates, are the second dominant lithology. Reworked coral, stromatoporoid, brachiopod, and crinoid debris is abundant in the detrital fractions. Successions of alternating fossil-impoveryed very thin-bedded micrites and marly shales, 1.3 m thick, form the uppermost part of set C (in this paper termed the Śluchowice Marly Level; see below). This level is characterized by appearance of pyrite and numerous lingulid brachiopods. The total thickness of the reef-proximal succession is 7.8 m. Thin-bedded bituminous micrites with many fossiliferous, coarse-grained and graded biointrarudite intercalations (up to 25 cm thick) are typical at the nearby WId-E section, where a ca. 9.5 m thick succession is developed.

At the composite WIE section, set C, ca. 8.5 m thick (Fig. 7), comprises rhythmically stratified, platy bituminous calcilutites and marly shale partings, which in places are wavy-bedded. Thin layers of intraclastic biorudites occur sporadically as well, but graded fossil-rich layers with brachiopods and crinoids are limited principally to the lower part of section (Fig. 7A). Abundant styliolinids appear in the uppermost, thin-bedded part, 1.7 m thick (Fig. 7B).

Set D is very well exposed in sections WId-W and WIE, where it also exhibits lateral disparity. Overall, at the WId-W section it is distinguished by the appearance of thick-bedded, light-coloured calcirudites with redeposited reef-builders, but renalcid-*Stachyodes* buildups occur as well. In addition, alternating thin-bedded, poorly fossiliferous micrites and shales (with styliolinids in places; Skwarek 1990) occur as subordinate partings.

Set D splits eastward into D₁ and D₂ subsets at the distal WIE section. The thin-bedded subset D₁ (about 7 m thick) is a transitional unit between set C and D, as defined by Szulczewski (1971), while the thick layers of subset D₂ corresponds well with set D of the WId-W section. Sharp lateral variations of thickness and lithology are unique features of the bottom part of this subset (beds no. 169 to no. 183; Fig. 7C, D); thicker micritic and detrital, partly conglomeratic, layers present at the southern part of the wall disappear abruptly over a distance of 10 m toward north, where thin-

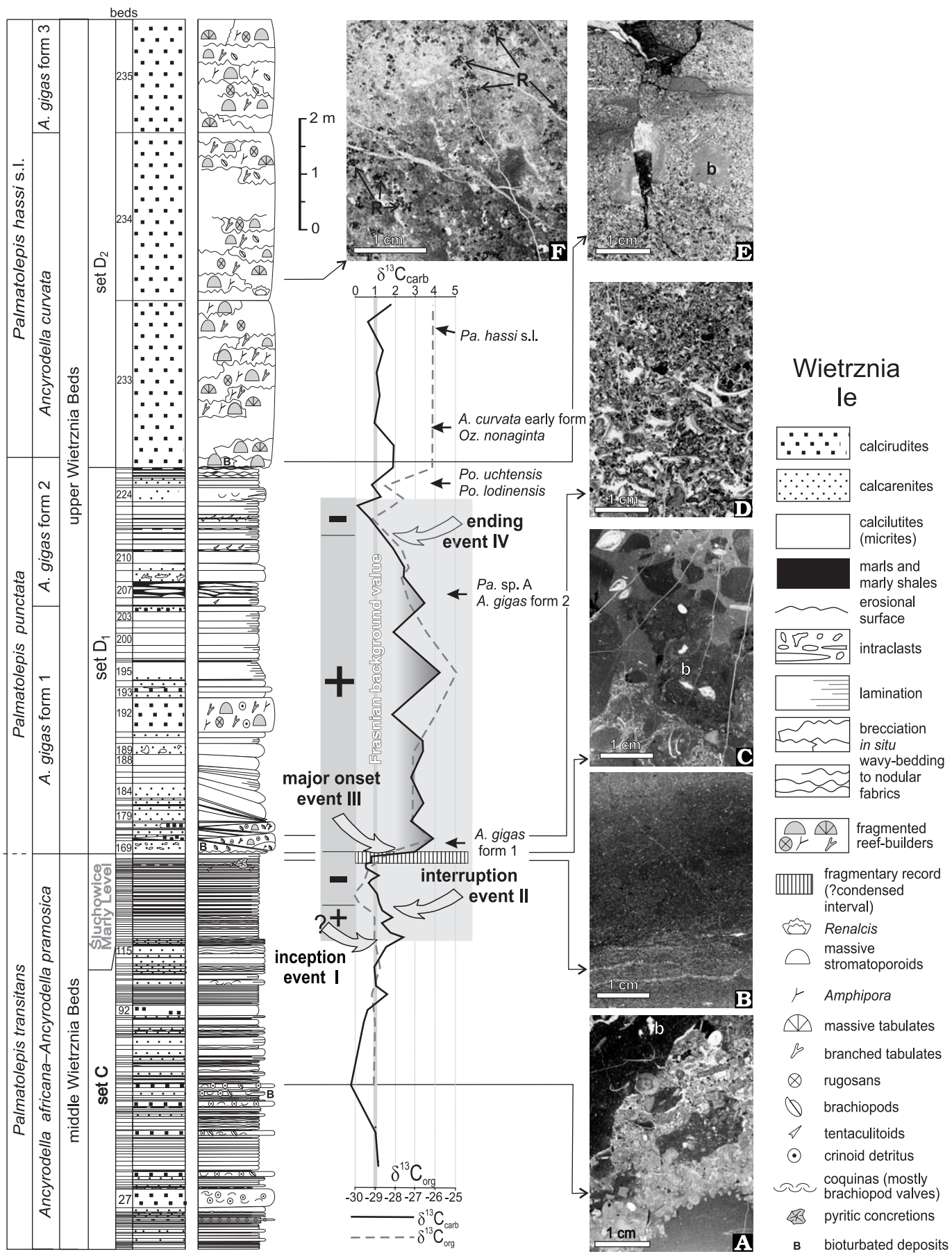
bedded micrites intercalated with shales are observed. Platy calcilutites and calcarenites, mostly laminated, are common higher in the succession. This unit is also characterized by increasing frequency of clay-rich and knobby intercalations toward its top. Fossils are absent, except broken reef-builders in one detrital layer and styliolinids in a few horizons in the upper part of the subset D₁. Unit D₂ comprises thick-bedded massive detrital light-coloured limestones with many intraclasts and fragmented reef-builders (stromatoporoids, corals, algae), brachiopods and crinoids, but also renalcid thrombolites (Fig. 7E, F).

The middle Wietrzna Beds were episodically deposited on the northern, storm-affected flank of the Kielce carbonate platform (Fig. 3). They comprise both coarse-grained, proximal tempestite layers (i.e., mostly episodic, storm-generated sediment-gravity flows from the Dyminy Reef margin) and micritic-marly (basinal) sediments (see the Transitional Facies of Szulczewski 1971; Vierek in press); the latter “background” lithofacies represents distal muddy tempestites rich in fine algal detritus (Skwarek 1990). The region was affected by synsedimentary tectonic activity (Racki and Narkevitch 2000), recorded in a drastically different, locally somewhat condensed stratigraphic succession of the E–MF boundary beds in adjacent tectonic blocks recognized to the east, in the middle part of the Wierzna exposure (section C of Dzik 2002: fig. 1; see Szulczewski 1989; Lamarche et al. 2003). At WIE section, the above-mentioned suite of rapidly wedging and differentiated basal layers of subset D₂, including flat-pebble conglomerates with a unique micritic matrix (Fig. 7C), as well as localized *in situ* brecciation of mostly higher massive layers (Fig. 7E), are seen as sedimentary signature of the tectono-seismic activity; a similar depositional phenomena in stratigraphically younger Late Devonian strata are described in Szulczewski (1968, 1971). Middle Frasnian deposition of the upper Wietrzna beds is marked by talus-like sediments in the upper foreslope setting, locally with a significant microbial and/or *Stachyodes*-dominated contribution to localized framework accretion and sediment baffling (see Bednarczyk et al. 1997).

Other sections analyzed

Śluchowice (Fig. 9).—The famous inactive Śluchowice (or Ślichowice) quarry, preserved as the Jan Czarnocki Geological Reserve, is located in the northwestern part of Kielce, and exposes spectacularly folded Frasnian strata of the northern Kielce Syncline, deposited in mostly deeper water facies (“Łysogóry facies” after Szulczewski 1971). The E–MF interval was studied on the north-western side of the partly covered eastern excavation, where an overturned fold occurs (Fig. 5A).

The lowest portion of the investigated succession (0.8 m) comprises alternating marly limestones and shales, with the rhynchonellid brachiopod *Phlogioiderhynchus polonicus* (Roemer, 1866), comparable to the Szydłówek Beds. How-



ever, due to poor exposure, this set was assigned with reservations to the Wietrzna Beds (set A) after Racki and Bütyncz (1993). According to these authors, this unit displays a transitional character due to irregular alternation of marly and coral-bearing detrital lithologies in the western Śluchowice quarry and nearby Czarnów hill (see figs. 2 and 4 in Racki and Bütyncz 1993; and fig. 1C, D in Racki and Sobstel 2004). The middle part (set B) consists of coarse-bedded intraformational conglomerates with calcarenite interbeds (Detrital Facies of Szulczeński 1968, 1971), both with abundant reworked reef-building fauna of the lower Wietrzna Beds (Racki and Bütyncz 1993); autochthonous stromatoporoid reef partings are found as well (Racki and Sobstel 2004). Early slump deformation is a marked feature in distinctively very thin-bedded, enriched by pyrite, fossil-impoverished marly unit pebbles (Fig. 5B), 1.3 m thick, occurring in the basal part of the Kostomłoty Beds and distinguished informally herein as the Śluchowice Marly Level. Overlying limestone layers include sparse rubble of corals and stromatoporoids (in the basal part only), as well as occasional brachiopods and crinoid detritus (Szulczeński 1971). In the upper part of the measured section, micrites with shaly and detrital intercalations dominate. Except for one styliolinid-rich horizon, fossils are absent in this part of succession. Detrital, partly conglomeratic layers with brachiopods and crinoids are present at the top of the section. This unit is characterized by abrupt lateral variation in thickness, probably resulting mostly from erosional channel filling (see Szulczeński 1968).

Kostomłoty-Mogiłki (Fig. 10).—A succession of dark-coloured micrites with shaly and detrital intercalations, in-part strongly tectonically disturbed, is well exposed in the small inactive quarry Kostomłoty-Mogiłki (= Kostomłoty-V, Fig. 4A; Racki et al. 2004), located a few kilometres NNE of Kielce, within the Miedziana Góra Syncline (Szulczeński 1971, 1981). This readily accessed outcrop is surprisingly poorly studied when compared with the active western Kostomłoty quarries (Racki et al. 1985, 2004; Racki and Bütyncz 1993).

The lowermost portion of the studied Frasnian section is characterized by intercalations of marly limestones and marly shales with nodule horizons and numerous detrital beds, representing the upper part of the Szydłówek Beds (see Racki and Bütyncz 1993; Borcuch 2006). The unit includes brachiopods

(*Phlogiderhynchus polonicus*, mostly as shelly debris), tabulate corals (abundant auloporids in the lowermost marly interbeds), crinoid detritus and styliolinids (*Styliolina* Horizon), but not the distinctive pyritic Goniatite Level, which is recognized only at the westerly Małe Górkí quarry (see Racki et al. 2004). The first thicker (about 0.5 m) coarse-detrital conglomerate beds, overlain by an arenite layer, define the bottom of the Kostomłoty Beds, as proposed by Racki et al. (1985). The Kostomłoty Beds comprise mainly fossil-poor micrites and marly limestones with a few coarse-grained intraclastic layers (Fig. 4B) and shaly intercalations (organic-rich in beds 100, 111, 114, 115, 116, 118). A bipartite succession of the higher, clay-rich Kostomłoty Beds at Kostomłoty-Mogiłki is evidenced by dominant wavy-bedded (beds no. 73 to no. 118) and nodular horizons with basal conglomeratic intercalations (beds above no. 118) in the lower and upper parts, respectively. Pyrite-rich horizons separate these two intervals.

Both the Szydłówek Beds and the Kostomłoty Beds represent the deeper water basin setting with mostly oxygen-depleted bottom conditions of the Kostomłoty transitional facies zone (Basin Facies of Szulczeński 1971; Racki and Bütyncz 1993; Racki et al. 2004).

Kowala-railroad cut (Fig. 11).—A section of the Frasnian limestones, exposed along the cut of Kielce-Busko railway, is located at the eastern part of the Gałęzice Syncline. Szulczeński (1971) has subdivided the continuous Late Devonian section into 8 lithological sets (A–H), and our E–MF investigations are scoped on the interval including the highest part of set B up to the lowest part of set F.

The set B consists of dark, wavy-bedded and coral-rich biostromal limestones with distinguishing shaly intercalations of the uppermost Kowala Formation (Narkiewicz et al. 1990). The set C includes light-coloured, bindstone-type biohermal limestones with stromatoporoid-coral associations (Kadzielnia-type mud-mounds; see Szulczeński and Racki 1981; Racki 1993b). Grey, micritic, brachiopod-bearing limestones are typical of set D (*Phlogiderhynchus* Level of Racki 1993b). Black marly interbeds occur exclusively in the lowermost part of this set. Szulczeński (1989) suggested that a stratigraphic gap and condensed bed (“initial stage”) occur at the bottom of set D, which records IIc flooding of the southern Kielce carbonate platform (Racki 1993b). The overlying set E is formed by thick micritic and detrital limestones with redeposited stromatoporoids and corals, as well

← Fig. 7. Lithology, conodont biostratigraphy (arrowed are first appearances of key taxa), microfacies (A–E) and stable carbon isotope geochemistry (both carbonates and organic matter; the results in per mil deviation from the Vienna Peepee Belemnite standard, VPDB) for the Early to Middle Frasnian strata at the reference Wietrzna Ie section in Kielce (see Figs. 3–6); lower parts of the succession, outcropped in the more eastern fragment of the wall, are omitted (see Figs. 6, 16). The boundary between *Ancyrodella rugosa* and *A. africana*–*A. pramosica* levels is accepted after Bütyncz and Racki (1993), but correlated with the *Mesotaxis falsiovalis*–*Palmatolepis transitans* zonal boundary (see Fig. 15). The geochemical anomaly interval is marked as grey interval, subdivided in positive (+) and negative (−) parts determined by four isotopic events I–IV. The conclusive proof of the distinctive positive $\delta^{13}\text{C}$ excursion (major event III), initially interrupted by fall late in the *Palmatolepis transitans* Zone, is provided by organic matter data. Note poorly laminated algal or styliolinid biomicrite background microfacies (A, B) and sparry (A, D) and micritic (C) detrital varieties, followed by *in situ* brecciated (E) graded intrasarenite and *Renalcis* boundstone (F). Abbreviations: b, burrows; R, *Renalcis* clumps; A., *Ancyrodella*; A. *afr.*–*A. pr.*, *Ancyrodella africana*–*A. pramosica* conodont level; Oz., *Ozarkodina*; Pa., *Palmatolepis*; Po., *Polygnathus*.

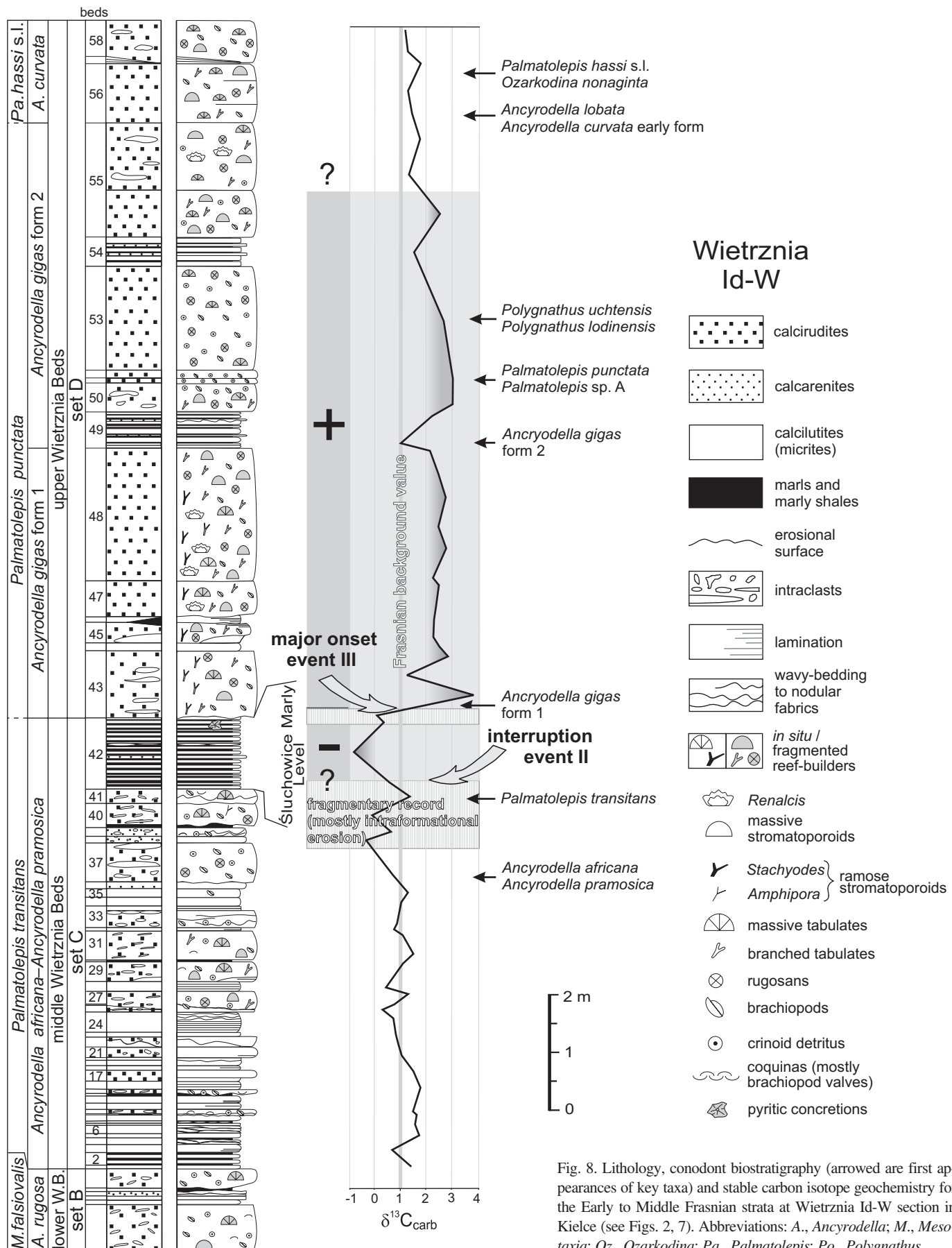


Fig. 8. Lithology, conodont biostratigraphy (arrowed are first appearances of key taxa) and stable carbon isotope geochemistry for the Early to Middle Frasnian strata at Wietrznia Id-W section in Kielce (see Figs. 2, 7). Abbreviations: A., Ancyrodella; M., Mesotaxia; Oz., Ozarkodina; Pa., Palmatolepis; Po., Polygnathus.

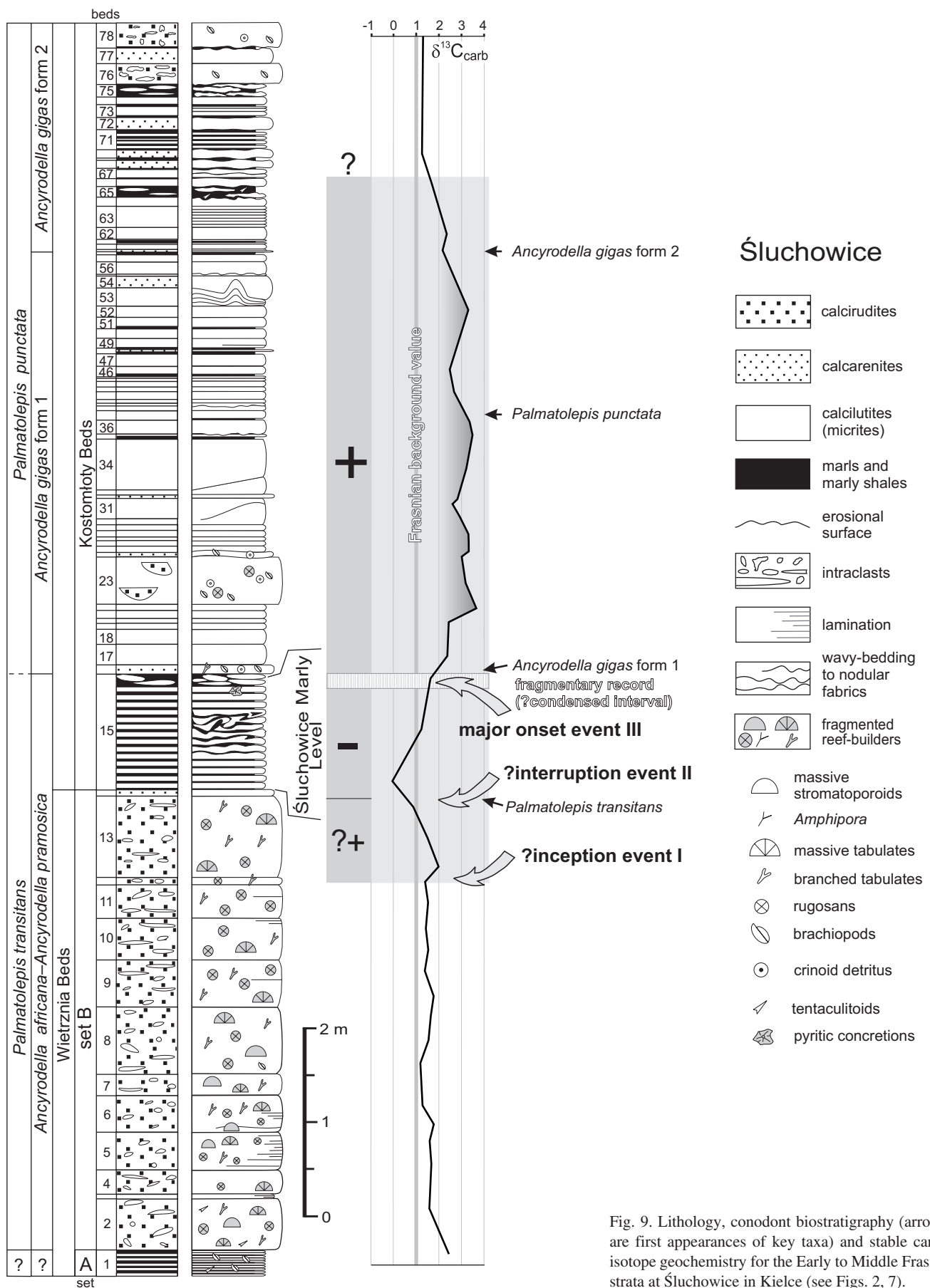


Fig. 9. Lithology, conodont biostratigraphy (arrowed are first appearances of key taxa) and stable carbon isotope geochemistry for the Early to Middle Frasnian strata at Śluchowice in Kielce (see Figs. 2, 7).

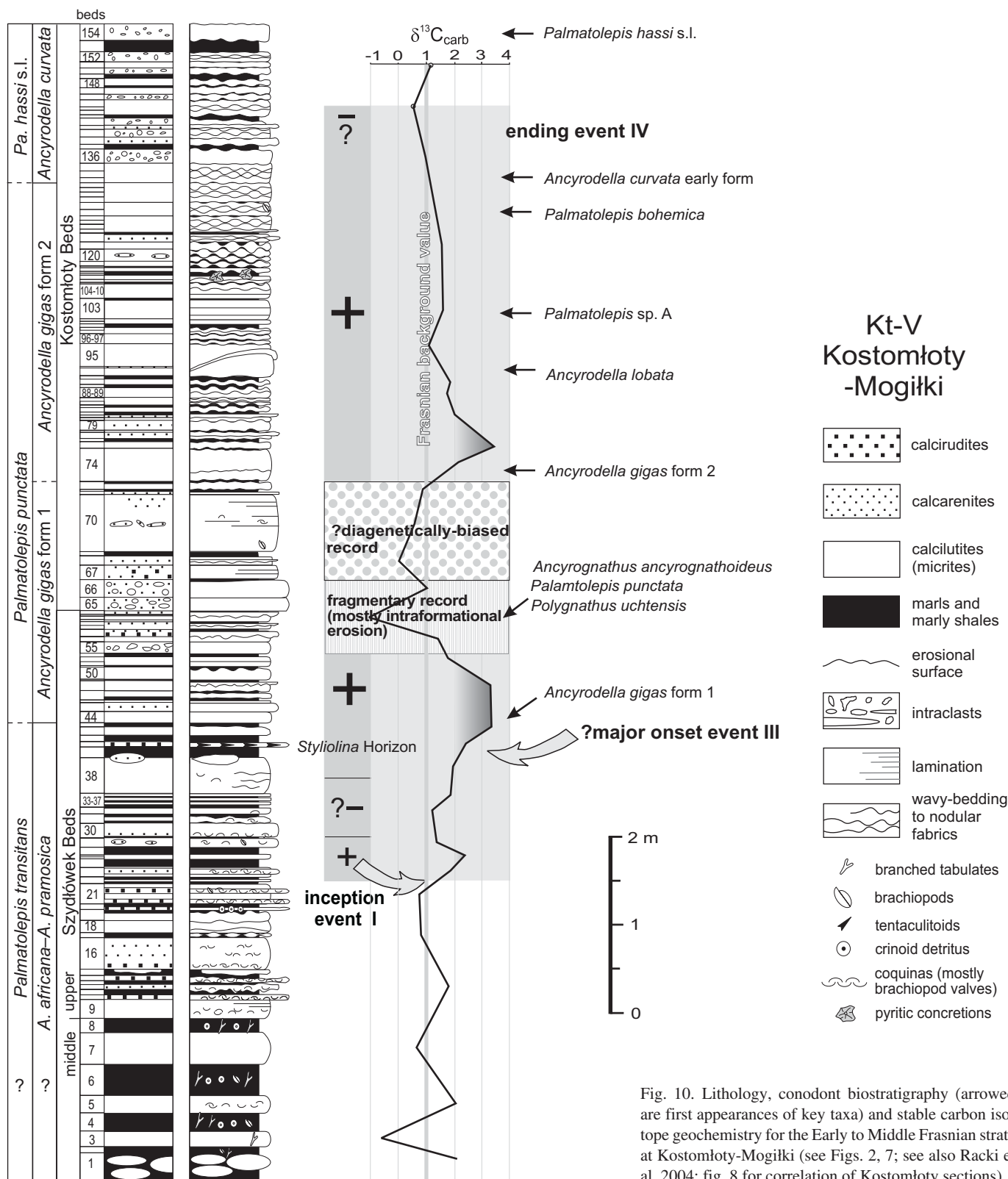


Fig. 10. Lithology, conodont biostratigraphy (arrowed are first appearances of key taxa) and stable carbon isotope geochemistry for the Early to Middle Frasnian strata at Kostomłoty-Mogiłki (see Figs. 2, 7; see also Racki et al. 2004: fig. 8 for correlation of Kostomłoty sections).

as by intraformational conglomerates (Detrital Facies of Szulczeński 1968, 1971). Thin-bedded, marly limestone and shales with tentaculitoids and rhynchonellid brachiopods (set F; see Szulczeński 1971: 75; Sartenaer et al. 1998) appear in the uppermost part of studied section. Slump deformation oc-

curs in both sets E and F. The folds in set E are sporadically broken and overlain by cross-bedded detrital reef sediments, however, isoclinal folds with isolated, limestone blocks enclosed by shales are present in the set F (Szulczeński 1968: figs. 2, 3).

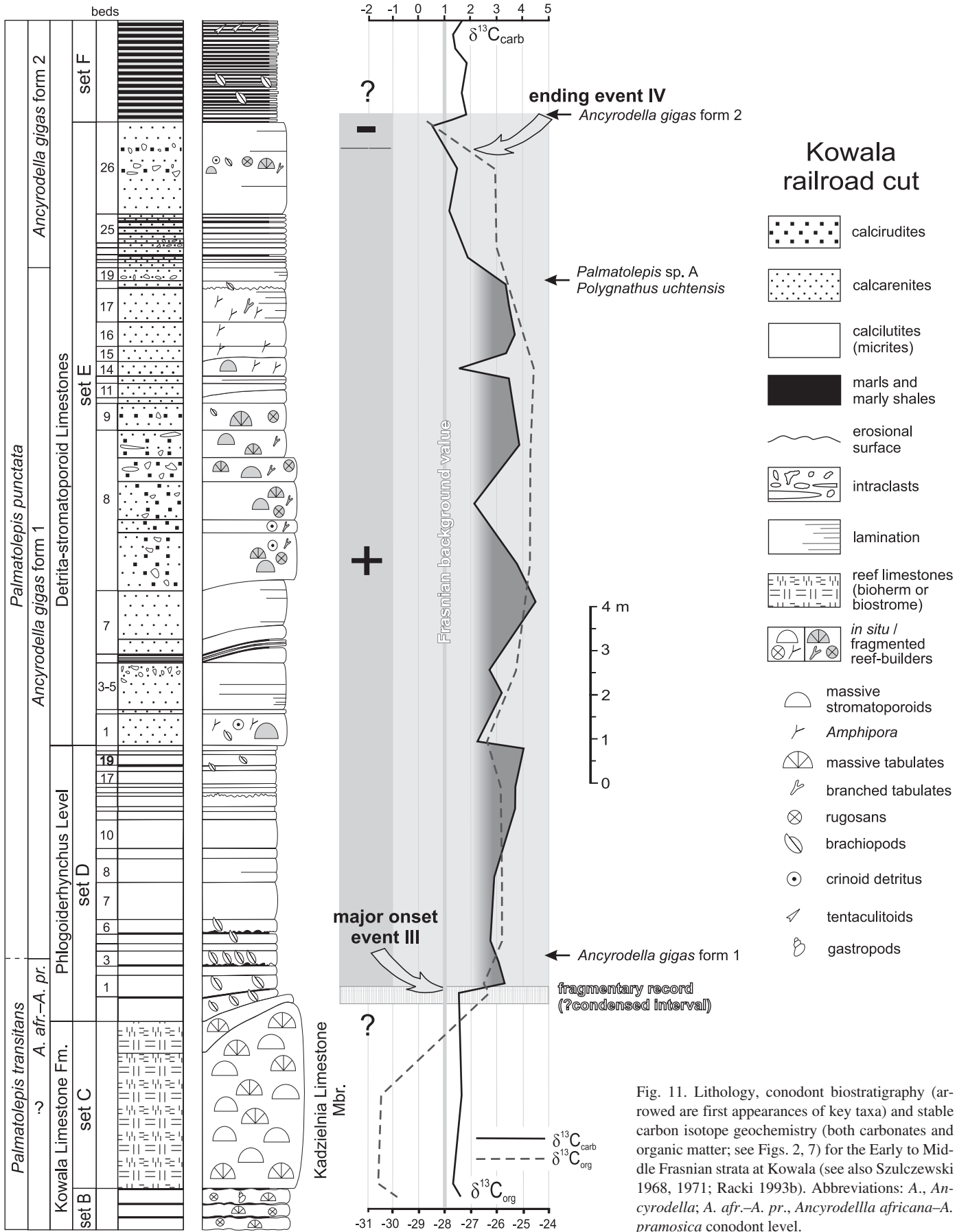
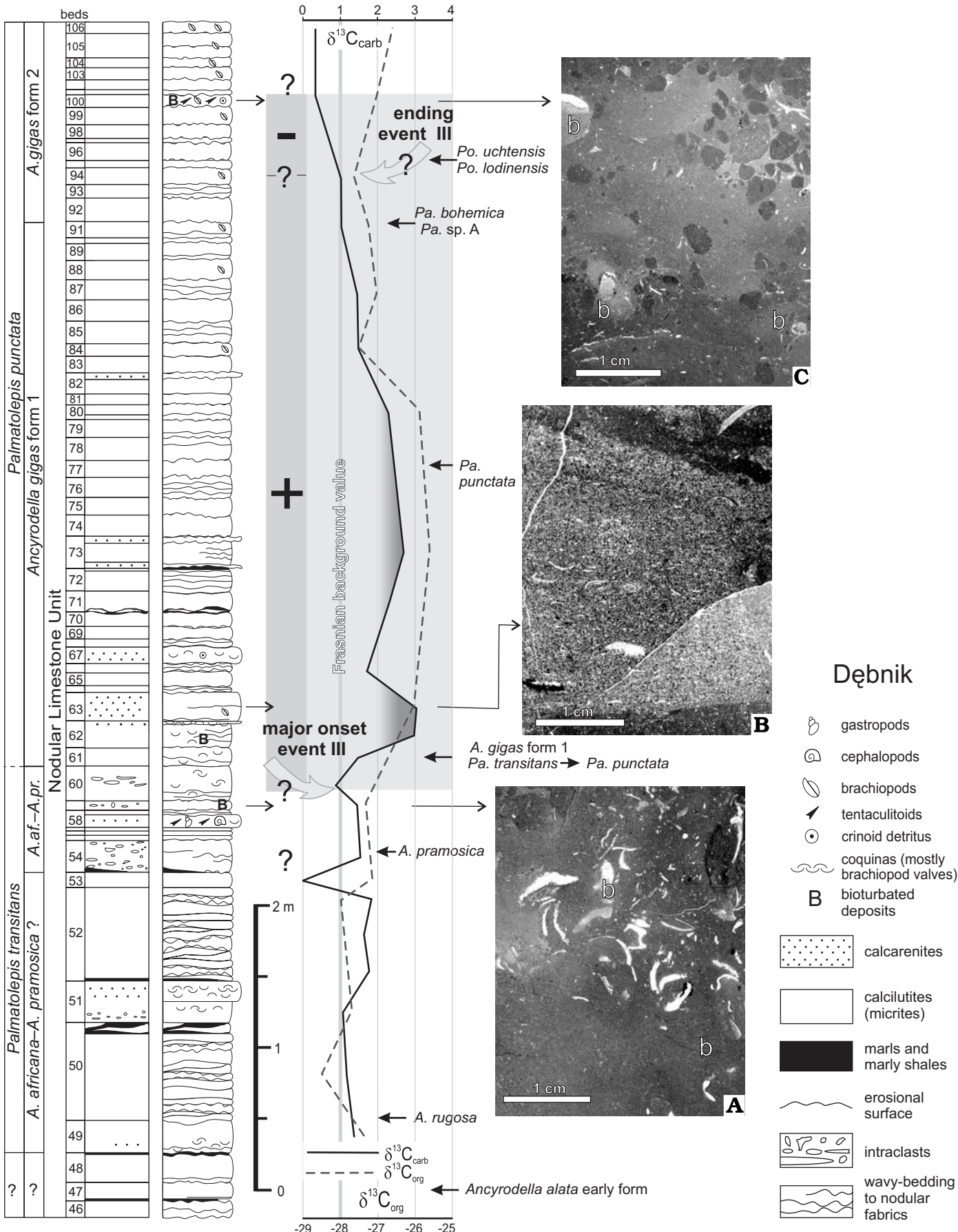


Fig. 11. Lithology, conodont biostratigraphy (arrowed are first appearances of key taxa) and stable carbon isotope geochemistry (both carbonates and organic matter; see Figs. 2, 7) for the Early to Middle Frasnian strata at Kowala (see also Szulczewski 1968, 1971; Racki 1993b). Abbreviations: A., *Ancyrodella*; A. afr.-A. pr., *Ancyrodella africana*-*A. pramosica* conodont level.



Dębnik (Fig. 12).—A small inactive quarry is located within the Dębnik Ridge at Dębnik village near Krzeszowice. Bałiński (1979, 1995) called this outcrop the “quarry above the Rokiczany Dół ravine”.

The studied section is situated in the western part of the quarry, and the monotonous succession is strongly dominated by thin-bedded marly micrites with clay-enriched intercalations. Additionally, sparse calcirudites and varieties with darker micritic intraclasts as well as styliolinid-rich horizon are found in the lower part of the section. The limestone succession has a typically wavy-bedded to nodular appearance and Narkiewicz and Racki (1984) assigned this set to the Nodular Limestone. Its sparse fossil association includes mostly debris of brachiopods, gastropods and crinoids in few layers.

Quiet-water deposition of the nodular-type calcareous sediments took place in the southern, proximal part of the gradually deepening Frasnian shelf basin transitional to a carbonate ramp (Narkiewicz and Racki 1987; Narkiewicz 1996), marked by reduced sedimentation rates and depositional hiatuses (Bednarczyk 1990).

Conodont material

A total of 265 samples were collected for conodont studies, and only 181 of them yielded conodonts. The weight of each sample was 0.7–1.5 kg. Among them, only the platform (Pa) elements (approximately 10,000 specimens; Tables 1–7 in Appendix 1) were used for biostratigraphical interpretations (see Figs. 13, 14). The state of preservation is generally good and even perfect in many samples of the upper parts of studied Frasnian interval. Conodont elements are most abundant at the Wietrzna and Kostomłoty exposures. The most productive samples are derived from detrital, mostly crinoid-brachiopod bioclastic layers of Wietrzna (up to 300 Pa elements in samples WId-W10 and WId-W11) in contrast to micritic intervals almost barren of conodonts (Makowska 2001; Sobstel et al. 2006). In other sections, bioclastic intercalations are also more conodont rich than the dominant micritic intervals (e.g., samples 62 in Dębnik, 21 in Kostomłoty), but there are exceptions, such as the micritic sample Kt-V 61, yielding 400 Pa elements.

Conodonts recovered from the Early–Middle Frasnian boundary interval in the Holy Cross Mountains and Silesia–Cracow sections are diverse and relatively abundant (e.g.,

Szulczeński 1971; Narkiewicz 1978; Bałiński 1979; Narkiewicz and Racki 1984; Sobstel 2003). However, the correlation of the studied sections with the standard conodont biozonation of Ziegler and Sandberg (1990) is rather difficult due to the absence of zonally important index palmatolepid species, i.e., *Palmatolepis transitans* Müller, 1956 and *Palmatolepis punctata* Hinde, 1879, representing deeper water biofacies. Conodont associations from this zonal transition are dominated by polygnathid and/or polygnathid-ancyrodellid fauna (Racki and Bultynck 1993; Sobstel et al. 2006). Only the latter ones are of a high biochronological value and are abundantly represented throughout the studied Early and Middle Frasnian carbonate rocks. Thus, the identification of zonal boundaries is based on species of *Ancyrodella* mainly (Fig. 15). The younger *Pa. punctata* Zone–*Pa. hassi* Zone boundary interval is represented by conodont associations enriched with palmatolepids, however, it seems also that the entry of zonal-index species (*Palmatolepis hassi* Müller and Müller, 1957) is delayed in many successions, as shown for older guide palmatolepid species by Racki and Bultynck (1993).

Nevertheless, zonal identification follows the scheme of Ziegler and Sandberg (1990), but it has been compared also with the alternative Montagne Noire (MN) zonation of Klapper (1988; for correlation of the two zonations, see Klapper and Becker 1999) and its equivalents from western Canada (Klapper and Lane 1989; Klapper 1997) and the Timan–Pechora region (Klapper et al. 1996; Ovnatanova et al. 1999; see Fig. 15). Moreover, the MN zonation allowed recognition of distinctive lower and upper *Pa. punctata* conodont faunas, and consequently divides the *Pa. punctata* Zone into two subzones. Additionally, stratigraphic ranges of many polygnathids were correlated with the polygnathid succession of the Russian Platform (Ziegler et al. 2000; Ovnatanova and Kononova 2001; Fig. 15). The comparison with the polygnathid scale of Ovnatanova and Kononova (2001) appeared to be particularly helpful, and, by many similarities, it proved its practical biostratigraphical application in the Polish sections. The oldest akyrodellid associations are easily compared to the ones described previously from the Early Frasnian of the Holy Cross Mountains by Racki and Bultynck (1993; see also Boruch 2006).

Four distinctive akyrodellid levels are distinguished throughout the *Pa. transitans*–*Pa. hassi* interval in the Holy Cross Mountains and Silesian Region (see Tables 1–7; Figs. 7–12): *Ancyrodella africana*–*A. pramosica* assigned to the *Pa. transitans* Zone (see Racki and Bultynck 1993), *A. gigas* form 1 and *A. gigas* form 2 belonging to the *Pa. punctata* Zone and *A. curvata* (early form) in the lowermost part of *Pa. hassi* s.l. Zone. The distinguished akyrodellid levels can be correlated approximately with the *Ancyrodella* zonation of Dzik (2002) from the Holy Cross Mountains, which for the first time was based on apparatus taxonomy; they embrace *A. rotundiloba*, *A. alata*, and lower part of *A. rugosa* zones of this author.

← Fig. 12. Lithology, conodont biostratigraphy (arrowed are first appearances of key taxa), representative microfacies (A–C) and stable carbon isotope geochemistry (both carbonates and organic matter; see Fig. 7) for the Early to Middle Frasnian strata at Dębnik near Cracow (see Fig. 1A). Note dominantly micritic, bioturbated microfacies (A, C) with burrows (b) and pseudo-intraclasts, rich in brachiopods (A; see also Racki and Bałiński 1981) and styliolinids (C), rarely intercalated with sorted biointrasparenate partings (B). Abbreviations: A., *Ancyrodella*; A. afr.–A. pr., *Ancyrodella africana*–*A. pramosica* conodont level; Pa., *Palmatolepis*; Po., *Polygnathus*.

Ancyrodella africana–Ancyrodella pramosica level.—The oldest diverse fauna is perfectly recorded in the lower part of Wietrznia and Kostomłoty sections, as noted already by Racki and Bultynck (1993). The Early Frasnian association is dominated by *Ancyrodella rugosa* Branson and Mehl, 1934 in Wietrznia (Fig. 13A) and *A. alata* Glenister and Klapper, 1966 (late form) in Kostomłoty, with the attendance of *A. rotundiloba* (Bryant, 1921), *A. recta* Kralick, 1994 and *A. triangulata* Kralick, 1994. The more evolutionarily advanced ancyrodellids, such as *A. africana* Garcia-Lopez, 1981 (Fig. 13C) and *A. pramosica* Perri and Spaletta, 1981 (Fig. 13B) are, however, rare or absent in lower part of set C in Wietrznia (Figs. 7, 8) so the assignment of the lower part of middle Wietrznia Beds to *A. africana–A. pramosica* ancyrodellid level is partly taken after Racki and Bultynck (1993). The more abundant *A. africana* and *A. pramosica* fauna enters higher, chiefly with the first *Palmatolepis transitans* and diversified mesotaxid species, i.e., *Mesotaxis falsiovalis* Sandberg, Ziegler, and Bultynck, 1989, *M. asymmetrica* (Bischoff and Ziegler, 1957), *M. bogoslovskyi* Ovnatanova and Kuzmin, 1991, and *M. costalliformis* (see Tables 1–4, 6), while the contribution of other ancyrodellids decreases significantly. The first appearance of the *A. africana–A. pramosica* fauna in Dębnik, in turn, coincides with the bloom of *Ancyrodella*, while the lower and higher portions of the succession are almost barren of ancyrodellids (Table 7). The lower part of the Dębnik section, although lacking unambiguous zonal indicators, has been assigned to the *A. africana–A. pramosica* level owing to the substantial biofacies change observed in other sections late in the *Pa. transitans* Zone and to chemostratigraphic indicators (Sobstel et al. 2006).

Among polygnathids the most important is *Polygnathus dubius* Hinde, 1879, with changing contributions of *Po. aequalis* Klapper and Lane, 1985 and *Po. decorosus* Stauffer, 1938. The other polygnathid taxa include *Po. dengleri* Bischoff and Ziegler, 1957, *Po. angustidiscus* Youngquist, 1947, *Po. pennatus* Hinde, 1879 and rare representatives of the *Po. webbi* group (morphological categories according to Ovnatanova and Kononova 2001 and Ji and Ziegler 1993; Tables 1–3), such as *Po. webbi* Stauffer, 1938 and *Po. alatus* Huddle, 1934. No significant changes among polygnathid associations are noted in this level, and any shift in their species composition seems to be facies controlled (see Sobstel et al. 2006). The last occurrence of *Po. dengleri*, which terminates in the *Pa. transitans* Zone, is within the *A. africana–A. pramosica* level in the Holy Cross Mountaints, in agreement with its total range elsewhere (e.g., Sandberg et al. 1989).

Specimens of *Klapperina*, mostly *K. ovalis* (Ziegler and Klapper, 1964), are encountered, as well as *Icriodus symmetricus* Branson and Mehl, 1934 and *I. expansus* Branson and Mehl, 1938. A relatively high contribution of *Icriodus symmetricus* is noted in the upper part of the *A. africana–A. pramosica* level. This species occurrences throughout the late *Pa. transitans* and *Pa. punctata* zones are marked by high frequency fluctuations, related to detrimental environ-

mental changes affecting its ecological niche (Sobstel et al. 2006; see also Fig. 18).

The distinctive duality of the *A. africana–A. pramosica* conodont interval with a rich ancyrodellid fauna in its lower part followed by diversified *Mesotaxis* and impoverished *Ancyrodella* populations may be compared to conodont assemblages from the topmost Early Frasnian South Timan sections (Ovnatanova et al. 1999; Becker et al 2001).

Ancyrodella gigas form 1 level.—The diverse ancyrodellid association is remarkably well represented by *Ancyrodella gigas* Youngquist, 1947 form 1 (*sensu* Klapper 1988; Fig. 13D, E), *A. africana*, *A. pramosica*, *A. recta*, and rare *A. triangulata*. Single *A. rugosa*, *A. rotundiloba*, and *A. soluta* are still present in the lowermost samples, however, they might be redeposited due to detrital nature of the limestones. Palmatolepids are almost absent, represented mostly by *Pa. transitans*, while the zone-defining *Pa. punctata* (Fig. 14K) is known only from the Kostomłoty and Śluchowice sections (see below).

The polygnathid fauna persists almost unchanged, still dominated by *Po. dubius* and *Po. decorosus*, although *Po. dengleri* is absent and *Po. pennatus* disappears in the lowermost samples. The set of new polygnathids, *Po. rudkinensis* Ovnatanova and Kononova, 1996 (Fig. 13M), *Po. uchtensis* Ovnatanova and Kuzmin, 1991 (Fig. 13P) and *Po. brevilamiformis* Ovnatanova, 1976 (Fig. 13R, S), appears abundantly only in Kostomłoty (Kt-V 61), while other new-comers, such as *Po. timanicus* Ovnatanova, 1969 (Fig. 13Q) and *Po. robustus* Klapper and Lane, 1985 (Deb 61), are rarely represented. The association is completed by *Klapperina ovalis*, *K. unilabius* (Huddle, 1981), *Mesotaxis asymmetrica*, and *M. falsiovalis*, as well as the same icriodid species pair (see below).

Ancyrodella gigas form 2 level.—Ancyrodellid diversity drops dramatically, and only *A. gigas* is present in the late *Pa. punctata* Zone. The species is represented by early and late forms, i.e., *A. gigas* form 1 and *A. gigas* form 2 of Klapper (1988; Fig. 13D, E, H, I). Sporadically, the emergence of *A. lobata* Branson and Mehl, 1934 higher up in this level is observed in the Kostomłoty area only (sample Kt-V 93). According to Klapper (1988) and Klapper et al. (1996), *A. gigas* form 2 is restricted to MN Zone 6, correlated with the late part of the *Pa. punctata* Zone (Klapper and Becker 1999; Kaufmann 2006; Fig. 15).

A change in ancyrodellid association occurs synchronously with the first appearance of *Pa. transitans* in the Wietrznia sections, together with rare *Pa. punctata* and a new palmatolepid fauna. This palmatolepid population shows a higher variety of morphological forms similar to the one described already by Kuzmin (1988) from Timan (Fig. 14A–C, E, F). According to Klapper and Foster (1993), the upper range of *Pa. transitans* is restricted to the middle–upper MN Zone 6. The new specimens transitional between *Pa. transitans* and *Pa. hassi* have been described as *Palmatolepis* sp. A (Fig. 14A–C). In the deeper water Kostomłoty succession

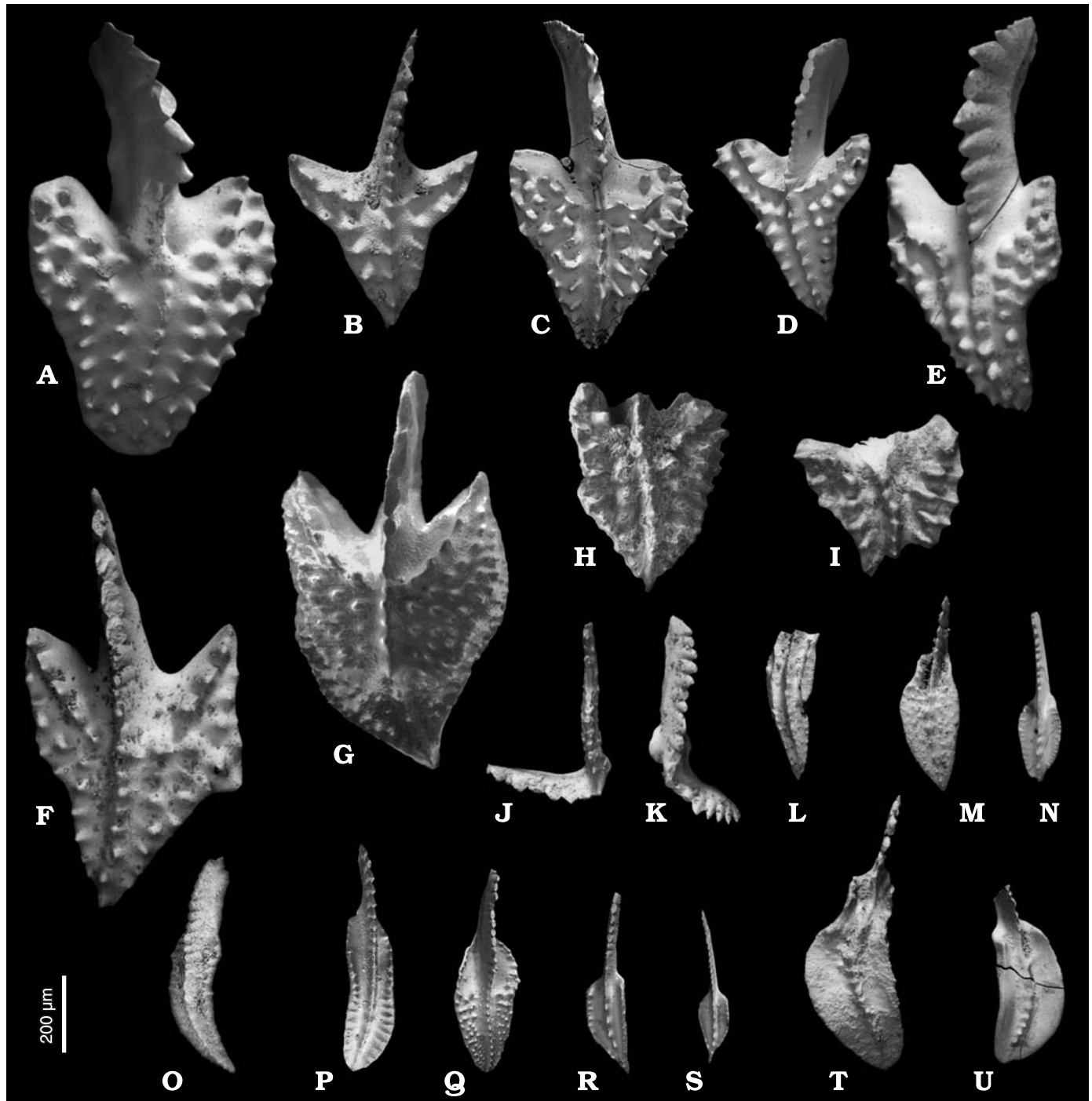


Fig. 13. Early to Middle Frasnian conodonts from the Holy Cross Mountains and Cracow region; SEM micrographs. **A.** *Ancyrodella rugosa* Branson and Mehl, 1934; GIUS 4-3428-1, sample Kt-V 21, Kostomłoty-Mogilki. **B.** *Ancyrodella pramosica* Perri and Spalletta, 1981; GIUS 4-3428-2, sample SI 17, Śluchowice. **C.** *Ancyrodella africana* Garcia-Lopez, 1981, GIUS 4-3428-3, sample WId-W 42/2, Wietrznia Id-W. **D, E.** *Ancyrodella gigas* Youngquist, 1947 (form 1 sensu Klapper, 1988). **D.** GIUS 4-3428-4, sample Deb 62B, narrow specimen showing affinities with *Ancyrodella pramosica*, Dębnik. **E.** GIUS 4-3429-1, sample WIe 169, Wietrznia Ie. **F.** *Ancyrodella curvata* (Branson and Mehl, 1934) early form, GIUS 4-3430-1, sample Kt-V 133, Kostomłoty-Mogilki. **G.** *Ancyrodella gigas* Youngquist, 1947 (form 3 sensu Klapper, 1988), GIUS 4-3431-1, sample WId-W 62, Wietrznia Id-W. **H, I.** *Ancyrodella gigas* Youngquist, 1947 (form 2 sensu Klapper, 1988). **H.** GIUS 4-3431-2, sample SI 89, Śluchowice. **I.** GIUS 4-3429-2, sample KPK F1, Kowala. **J.** *Ozarkodina nonaginta* Klapper, Kuzmin, and Ovnatanova, 1996, GIUS 4-3429-3, sample WIe 233/2, Wietrznia Ie. **K.** *Ozarkodina trepta* (Ziegler, 1958), GIUS 4-3430-2, sample Kt-V 128, Kostomłoty-Mogilki. **L.** *Polygnathus efimovae* Kononova, Alekseev, Barskov, and Reimers, 1996, GIUS 4-3429-4, sample KPK F1, Kowala. **M.** *Polygnathus rudkinensis* Ovnatanova and Kononova, 1996, GIUS 4-3429-5, sample Kt-V 61, Kostomłoty-Mogilki. **N.** *Polygnathus elegantulus* Klapper and Lane, 1985, GIUS 4-3429-6, sample KPK F1 Kowala. **O.** *Polygnathus lodinensis*, Pölsler, 1959, GIUS 4-3428-5, sample WId-W 50/2, Wietrznia Id-W. **P.** *Polygnathus uchtensis* Ovnatanova and Kuzmin, 1991, GIUS 4-3429-7, sample Deb 94, Dębnik. **Q.** *Polygnathus timanicus* Ovnatanova, 1969, GIUS 4-3429-8, sample Deb 61, Dębnik. **R, S.** *Polygnathus brevilamiformis*, Ovnatanova, 1976, GIUS 4-3429-13 (R) and GIUS 4-3429-14 (S), sample KPK F1, Kowala. **T, U.** *Polygnathus zinaiidae* Kononova, Alekseev, Barskov, and Reimers, 1996, GIUS 4-3429-9 (T) and GIUS 4-3429-10 (U), sample WIe 233/4, Wietrznia Ie.

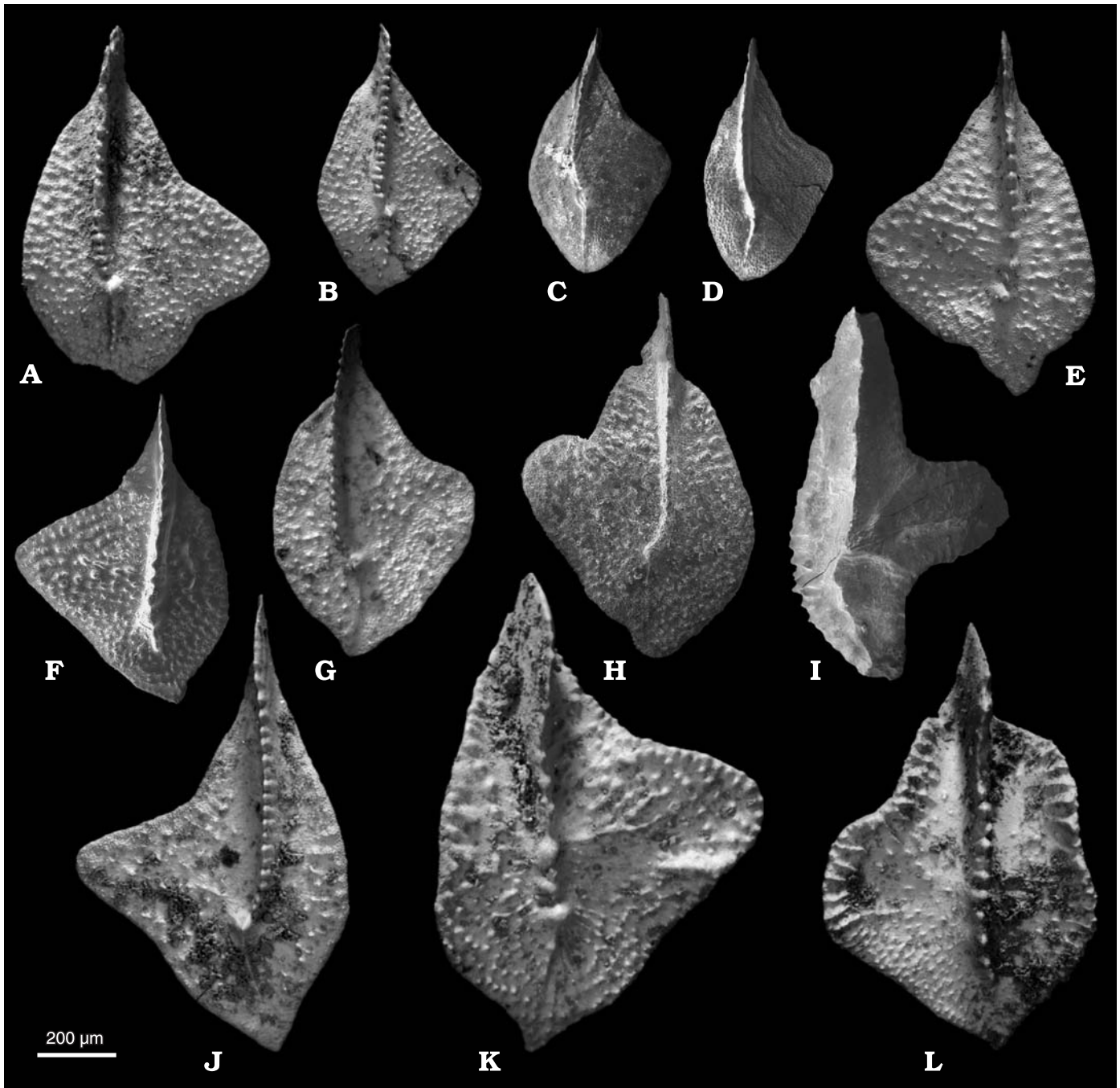


Fig. 14. Palmatolepids (A–H, J–L) and ancyrognathids (I) from Middle Frasnian of the Holy Cross Mountains and Dębnik; SEM micrographs. **A–C** *Palmatolepis* sp. A. A. GIUS 4-3428-6, sample KPK F1, Kowala. B, C. GIUS 4-3429-11 (B) and GIUS 4-3431-3 (C), sample Kt-V 128, Kostomłoty-Mogilki. All specimens are characterized by the platform outline transitional between *Palmatolepis transitans* and *Palmatolepis hassi*. They possess slightly curved carina and laterally directed outer lobe demarcated by weak to moderate sinuses. The platform is nearly flat, poorly ornamented or covered with fine nodes. Some specimens (C) show affinities to *Palmatolepis gutta* Kuzmin, 1998, however, the wider platform of *Palmatolepis* sp. A has more pronounced, triangular outer lobe. From *Palmatolepis punctata* they differ in uniform and more delicate ornamentation and a sinuous course of carina, however the posterior carina is not as much curved inward as in *Palmatolepis hassi*. **D, J**. *Palmatolepis hassi* Müller and Müller, 1957 (*sensu* Ziegler and Sandberg, 1990). **D**. GIUS 4-3431-4, sample WId-W 62, Wietrznia Id-W. **J**. GIUS 4-3432-1, sample Kt-V 154, Kostomłoty-Mogilki. **E**. *Palmatolepis* sp., GIUS 4-3428-7, sample Wle 233/2, Wietrznia Ie, specimen displaying similarity to *Pa. maximovae* Kuzmin, 1998 with its deep sinus in posterior part of the platform. **F**. *Palmatolepis* aff. *triquetra* Kuzmin, 1998, GIUS 4-3432-2, sample KPK F9, Kowala. **G**. *Palmatolepis plana* Ziegler and Sandberg, 1990, GIUS 4-3429-12, sample Wle 233/2, Wietrznia Ie. **H**. *Palmatolepis* aff. *Pa. proversa* Ziegler, 1958, GIUS 4-3432-3, sample WId-W62, Wietrznia Id-W. **I**. *Ancyrognathus* sp. A, GIUS 4-3432-4, sample SI 16, Śluchowice. The Pa elements of the specimens are robust, covered irregularly with nodes or short transverse ridges on marginal sides; posterior carina is gently curved outwardly while secondary carina is slightly directed anteriorly; pit is large, elongated and diamond-shaped. **K**. *Palmatolepis punctata* (Hinde, 1879), GIUS 4-3428-8, sample Kt-V 128, Kostomłoty-Mogilki. **L**. *Palmatolepis bohemica* Klapper and Foster, 1993, GIUS 4-3430-3, sample Kt-V 128, Kostomłoty-Mogilki.

Subage	Standard Conodont Zones (SCZ) (Ziegler and Sandberg 1990)	MN Zones (Klapper 1988)	Conodont succession in Holy Cross Mts. (Racki and Bultynck 1993; this paper)	Conodont succession in Ardennes modified by graphic correlation (Gouwy and Bultynck 2000)	Conodont succession and events in Timan (Kuzmin et al. 1997 Klapper et al. 1997 Ovnatanova et al. 1999 Becker et al. 2001)	Conodont intervals in Middle Devonian Field (Zhuravlev et al. 2006)	Polygnathid zones of Central East European Platform (Ziegler et al. 2000; Ovnatanova and Kononova 2001)
Middle Frasnian	Early <i>Pa. hassi</i>	8 (<i>Pa. aff. Pa. proversa</i>)	<i>A. gigas</i> form 3	<i>Ag. coeni</i> – <i>Ag. tsiensi</i> <i>Pa. proversa</i> <i>A. curvata</i> – <i>Pa. plana</i>	<i>Pa. aff. Pa. proversa</i> – <i>Oz. nonaginta</i>	no fauna	<i>Po. efimovae</i>
		7 (<i>O. nonaginta</i>)	<i>A. curvata</i>	<i>Pa. punctata</i>	<i>Mesotaxis extinction</i> <i>Pa. bohemica</i>	<i>CI 5 Po. efimovae</i>	
	<i>Pa. punctata</i>	6 (<i>Ag. primus</i>)	<i>Mesotaxis extinction</i> <i>Pa. bohemica</i>	<i>Pa. punctata</i>	<i>Mesotaxis–Klapperina extinction</i>	<i>CI 4 Po. ilmenensis</i>	
		<i>A. gigas</i> form 2	<i>A. gigas</i> form 1	<i>A. lobata</i>	<i>Pa. bohemica</i> – <i>Pa. spinata</i>	<i>CI 3 Po. pollocki</i>	
		5 (<i>Pa. punctata</i>)		<i>Ag. aencyrognathoides</i>	<i>Mesotaxis extinction</i> <i>A. curvata</i> early <i>Pa. gutta</i> <i>M. johnsoni</i> – <i>Pa. maximovae</i> <i>Pa. punctata</i> – <i>A. gigas</i>	?	
	<i>Pa. transitans</i>	4 (<i>Pa. transitans</i>)	<i>Pa. transitans</i> – <i>M. bogoslovskyi</i> <i>A. africana</i> – <i>A. pramosica</i>	<i>Pa. transitans</i>	<i>Po. aequalis</i> – <i>Po. decorosus</i> <i>M. falsiovalis</i> – <i>A. gigas</i>	<i>CI 2 Po. xylus</i> – <i>Po. reimersi</i>	<i>Po. reimersi</i>
		3 (<i>A. rugosa</i>)	<i>A. rugosa</i>	<i>A. africana</i> – <i>A. pramosica</i> <i>A. rotundiloba</i>	<i>Pa. transitans</i>	?	
	<i>M. falsiovalis</i> (M. asymmetricus)	2 (<i>A. rotundiloba</i> late)	<i>A. rotundiloba</i>	<i>A. rugosa</i> – <i>K. ovalis</i>	<i>A. africana</i>	<i>CI 1 Po. lanei</i>	<i>Po. alatus</i>
		Early (part)	1 (<i>A. rotundiloba</i> early)	<i>A. soluta</i> → <i>rotund.</i>	<i>Po. posterus</i> – <i>Po. Ijaschenkoi</i>	no fauna	
				<i>Late M. falsiovalis</i>	<i>A. alata</i> – <i>A. rugosa</i> <i>Po. xylus</i> – <i>Po. angustidiscus</i>		

Fig. 15. Correlation of “standard”, Montaigne Noire (MN) and several regional conodont zonal schemes and successions (the Ardenne succession compiled from Gouwy and Bultynck 2000: fig. 2); note different correlation of aencyrodellid-based units with standard zones. Abbreviations: *A.*, *Ancyrodella*; *Ag.*, *Aencyrognathus*; *K.*, *Klapperina*; *M.*, *Mesotaxis*; *Oz.*, *Ozarkodina*; *Pa.*, *Palmatolepis*; *Pl.*, *Playfordia*; *Po.*, *Polygnathus*.

(sample Kt-V 128), palmatolepids are abundantly represented by *Palmatolepis bohemica* Klapper and Foster, 1993 (= *Pa. plana* Ziegler and Sandberg, 1990, according to Ziegler and Sandberg, 2000; also present in Dębnik sample 92; Fig. 14L), whose entry is correlated with the upper part of MN Zone 6 (Klapper and Foster 1993, see also a reference conodont succession in South Timan in Becker et al. 2001, Fig. 15). In addition, the same sample includes *Ozarkodina trepta* (Ziegler, 1958) (Fig. 13K), the species known from MN Zone 6 again in the Montagne Noire and Timan-Pechora region (Klapper 1988; Klapper et al. 1996; Ovnatanova et al. 1999), although Ziegler and Sandberg (1990) show that the total range of *Ozarkodina trepta* is contained within the Early *Pa. hassi* Zone only.

Polygnathids are the most diversified in this level as compared to the whole interval under study. *Polygnathus timanicus*, *Po. uchtensis*, and *Po. brevilamiformis* have earlier entries at Kostomloty, but now they start to be richly represented in all other sections. Additionally, a significant shift between the long-ranging *Po. dubius* and *Po. webbi* groups coincides with the first appearance of *Ancyrodella gigas* form 2. *Po. dubius*-dominated faunas are replaced by the *Polygnathus webbi* group late in the *Pa. punctata* Zone.

Other biogeographically new polygnathids, *Po. lodinensis* Pölsler, 1969 (Fig. 13O) and the rarely represented *Po. efimovae* Kononova, Alekseev, Barskov, and Reimers, 1996 (Fig. 13L), arising in this level, were probably immigrants from the East European Platform. The former is a species widely distributed in basinal facies of the Volga and Timan-Pechora regions, and its first appearance approximates the base of the middle Domanik formation (= Early *Pa. hassi* Zone).

Zone), as well as in the Ardenne succession, while in the Rheinisches Schiefergebirge it appears before the *Pa. jamieae* Zone (Ziegler et al. 2000; Ovnatanova and Kononova 2001). The Kowala and Dębnik sites yield rare specimens of *Po. efimovae*, the zone-defining species of polygnathid zonation in the central region of the Russian Platform (Semiluki Horizon = *Pa. punctata* Zone–*Pa. jamieae* Zone interval; Ovnatanova and Kononova 2001). *Po. gracilis* is another polygnathid species appearing high within the aencyrodellid level in the Holy Cross sections. Importantly, the polygnathid succession of *Po. robustus*, *Po. elegantulus* Klapper and Lane, 1985 and, finally, *Po. gracilis* Klapper and Lane, 1985 has been recognized by Klapper and Lane (1985, 1989) in western Canada, and their first appearance sequence is confirmed in the Polish conodont succession.

***Ancyrodella curvata* level.**—The youngest conodont association is notably characterized by the first appearance of *Ancyrodella curvata* Branson and Mehl, 1934, early form, as is evidenced in the base of set D₂ of Wietrzna Ie (sample WIe 233/1), Wietrzna Id (WIe-W 56/1) and Kostomloty-Mogilki (Kt-V 133) (see Tables 1, 3, 6; Fig. 13F). This species entry in the Wietrzna succession is accompanied by *A. lobata*. Among palmatolepids, *Pa. plana* Ziegler and Sandberg, 1990 and sporadically *Pa. hassi* Müller and Müller, 1957 *sensu lato* (as defined by Ziegler and Sandberg, 1990; see Bultynck et al. 1998; Klapper and Becker 1999; Klapper and Foster 1993 for descriptions) appear in some sections (Tables 1, 3–6; Fig. 14D, G, J). The contribution of mesotaxids is significantly lower, while icriodids are invariably represented by *Icriodus symmetricus* and *I. expansus*, as well as a variety of polygnathids

from the *Polygnathus webbi*, *Po. uchtensis*, and *Po. xylus* groups. The association includes also *Ozarkodina nonaginta* Klapper, Kuzmin, and Ovnatanova, 1996 and *Po. zinaiidae* Kononova, Alekseev, Barskov, and Reimers, 1996 (Fig. 13T, U) as newly immigrating species.

According to Ziegler and Sandberg (1990), the first occurrence of *Ancyrodella curvata* indicates the base of *Palmatolepis hassi* Zone. However, Klapper (1988) noted an earlier entry of this species in MN Zone 6 (= the late part of the *Pa. punctata* Zone). The evidence of an Early *Pa. hassi* Zone assignment for the *A. curvata* level is additionally given by *Oz. nonaginta* (WIE 233/2, 233/4, 233/5; Fig. 13J); this is the guide species for MN Zone 7, which is correlated with the Early *Pa. hassi* Zone (Fig. 15; see also Klapper and Becker 1999). Among newly appearing polygnathids, *Po. zinaiidae* was described from the upper part of Semiluki and Voronezh Horizons of the Russian Platform (= *Pa. hassi*-Early *Pa. rhenana* zones), but is also known from the Franco-Belgian Basin (Early *Pa. hassi* Zone; Ziegler et al. 2000). *Pa. hassi* s.l. usually appears late (see Dzik 2002: 623), mainly within younger *A. curvata* association enriched with *A. gigas* form 3 (Fig. 13G) and *Palmatolepis* aff. *Pa. proversa* (Fig. 14H; WIE 235, WID-W 62). The latter species indicate the late part of Early *Pa. hassi* Zone (MN Zone 8; *Palmatolepis* aff. *Pa. proversa* itself is an index species for MN Zone 8, see Klapper and Becker 1999). According to Klapper (1988: 455), the first appearance of *A. gigas* form 3 is within the upper part of MN Zone 8. It seems that the first appearance of *Pa. hassi* is delayed in some areas due to facies interdependence of that species as was documented by Dzik (2002), especially when paired with overall low conodont frequency in this interval (Sobstel et al. 2006). The latest *Pa. punctata* Zone in the Kowala railroad cut (set F of Szulczeński 1971) is especially enriched with palmatolepids, while ancyrodellids are exceptionally rare, so the entry of *A. gigas* form 2 seems to be delayed at this locality. Szulczeński (1971) placed the *Pa. punctata*-*Pa. hassi* zonal boundary within the topmost part of the set E in Kowala, while our new conodont data point rather to a faunal shift in this interval only, connected with the transition from the *A. gigas* form 1 to *A. gigas* form 2 associations, and the first appearance of *Palmatolepis* sp. A instead of *Pa. hassi*.

The *Pa. punctata*-*Pa. hassi* zonal boundary at Wietrzna Id-W is recognized in the upper part of set D (sample WID-W 56; Fig. 8), according to data of Szulczeński (1971: 70–71, fig. 7). In the Wietrzna Ie section, however, this boundary is lowered to the base of subset D₂ instead of its middle part (Fig. 7), as it was suggested by Szulczeński (1971).

Early–Middle Frasnian boundary

As recommended by the SDS Frasnian Subdivisions Working Group for the Middle Frasnian substage base in a three-fold Frasnian subdivision (Becker and House 1998; Ziegler and Sandberg 2001), the base of the *Palmatolepis punctata* Zone

(Montagne Noire Zone 5) was proposed as the base of the Middle Frasnian. Thus, the first appearance of the widely distributed and widely recognized *Pa. punctata*, paired with the nearly concurrent appearance of *Ancyrodella gigas*, serves as a biostratigraphical marker that corresponds to the base of TR cycle IIc of Johnson et al. (1985), as well as the Middlesex deepening event in eastern North America (see <http://www.geneseo.edu/~frasnian/index.htm>). The conceptual link with this sea-level rise is an obvious step toward a natural subdivision of this stage (see Walliser 1985), effectively strengthened chemostratigraphically by discovery of the major perturbation of the global carbon budget, i.e., “*punctata* Isotopic Event” of Yans et al. in press (= *Pa. punctata* Event).

Ancyrodella gigas appears to be the key species for recognizing the base of the *Pa. punctata* Zone, and therefore the E–MF boundary, in our studied sections owing to the absence of index species within the *A. gigas* form 1 association. Generally, the first palmatolepids appear late in the *Pa. punctata* Zone, and the first occurrence of *Pa. punctata* coincides with the entry of more advanced species (*Palmatolepis* sp. A; Fig. 14A–C). As shown by Sandberg et al. (1989), the first occurrences of *P. punctata* and *A. gigas* are to some extent diachronous, which in the Holy Cross successions is clearly a matter of biofacies differentiation in most cases (Sobstel et al., 2006). Usually, the entry of *A. gigas* preceded slightly that of *Pa. punctata* (e.g., Klapper 1988). But, as is shown by graphic correlation (Gouwy and Bultynck 2000: fig. 2, table 1), the foregoing may even span the whole zone; in an extreme case, the first appearance of *A. gigas* may coincide with the base of the *Pa. transitans* Zone. Nonetheless, the co-occurrence of *Pa. punctata* and *A. gigas* is noted in the same samples at many localities around the world (Sandberg et al. 1994), and according to Ziegler and Sandberg (1990), their joint appearance, accompanied by the continued presence of *A. rotundiloba*, conclusively indicates the *Pa. punctata* Zone.

Conodont faunas associated with the first appearance of *Ancyrodella gigas* are significantly less diversified and more ancyrodellid-impoorer, belonging mostly to polygnathid biofacies (Tables 1–7; Sobstel et al. 2006). As noted above, the Dębnik locality is the exception, where this interval is connected with high ancyrodellid frequency (Fig. 12, Table 7). Thus, the transition from *A. africana*-*A. pramosica* to *A. gigas* faunas, and indirectly the position of the *Pa. transitans*-*Pa. punctata* zonal boundary, is best documented in the Dębnik section. There is no abrupt change in *Ancyrodella* associations at this interval, and the *A. africana*-*A. pramosica* association is smoothly replaced by the *A. gigas* fauna in the successive samples, accompanied by transitional forms from *A. africana* to *A. gigas* (samples Deb 61, Deb 62A). This gradual replacement is not observable at Wietrzna and Śluchowice, but is explainable by the conodont-barren Śluchowice Marly Level below the first *A. gigas* appearance, related to an overall conodont extermination (Sobstel et al. 2006; see also Fig. 18). At Dębnik, the stratigraphically oldest *A. gigas* form 1 enters together with a transitional form of *Pa. transitans* towards *Pa. punctata* (Deb 61) and bioge-

graphically new species *Polygnathus timanicus* and *Po. robustus*. The latter are known worldwide mostly from the *Palmatolepis punctata* and *Pa. hassi* zones (Szulczeński 1971; Klapper and Lane 1985, 1989; Ziegler et al. 2000), but probably originated late in the *Pa. transitans* Zone (Sandberg et al. 1989; Klapper and Lane 1989). *Po. timanicus* is a key species for recognition of the base of the *Pa. punctata* Zone in the Russian Platform, appearing almost synchronously with *Pa. punctata* (Kuzmin and Yatskov 1997; Ziegler et al. 2000) in the deep-water realm as an indicator of transgressive episode IIc of Johnson et al (1985).

The first occurrence of *A. gigas* form 1 in Kostomłoty-Mogilki (Kt-V 44) is found 1.2 metres below the appearance of *Pa. punctata* and new *Po. uchtensis*, *Po. rudkinensis*, and *Po. brevilamiformis* (Kt-V 61). The incoming polygnathid association from Kostomłoty also has a biochronological value. *Po. uchtensis* is a species known mostly from the *Pa. punctata*-*Pa. hassi* zonal interval in the deep-water Rheinisch and East European settings, although *Po. aff. uchtensis* may appear already in the *Pa. transitans* Zone (Ziegler et al 2000; Ovnatanova and Kononova 2001). The occurrence of *Po. rudkinensis* is surprising due to its endemic occurrence in the shallow-water Rudkino beds of the Russian Platform (Lower Semiluki Regional Stage of the Voronezh area; Ovnatanova and Kononova 2001). The Lower Semiluki Stage is correlated with the *Pa. punctata* Zone, so the restricted occurrence of *Po. rudkinensis* within this zone could be a good biostratigraphic indicator also in Poland. *Po. brevilamiformis* is another immigrant from the Russian Platform. It has its lowermost occurrence in the Lower Semilukian, and is later known also in the *Pa. hassi* Zone in the Franco-Belgian Basin and Rheinisches Schiefergebirge (Ziegler et al. 2000).

The specific conodont association of the sample Kt-V 61 is also characteristic for all other sections, but it emerges late in *Pa. punctata* Zone there, as it is indicated by the presence of *Ancyrodella gigas* form 2, however lacking in Kostomłoty. The earlier entry of this fauna in the deepest water Kostomłoty basin may be explained by biofacies control, although such a “conodont anomaly” is not detected in the adjacent, also deeper water, succession at Śluchowice.

Due to the absence of *Pa. punctata* in many sections (Wietrznia, Kowala, Śluchowice) the position of the Middle Frasnian base is tied with the entry of *A. gigas* especially as it is correlated with the carbon positive anomaly and initiation of IIc sea-level rise. This conclusion is recommended for consideration by the SDS.

High-resolution biostratigraphy versus chemostratigraphy

A large $\delta^{13}\text{C}_{\text{carb}}$ shift was unexpectedly discovered recently at the intra-zonal scale within the Early–Middle Frasnian transition, considered until recently as a biogeochemically and evolutionarily overall “quiescent” interval (see summary in

Racki 2005). A high stratigraphic resolution of the stable isotopic record, derived from well-dated, biostratigraphically continuous sections in the Ardennes, allowed detection of prominent positive-negative $\delta^{13}\text{C}_{\text{carb}}$ excursions (from 5.85‰ to -1.2‰) in the *Pa. punctata* Zone, preceded by an incipient positive shift in the *Pa. transitans* Zone, up to 4.1‰ (Cycle 6 in Yans et al. in press). High-resolution stable isotope data through the five Holy Cross Mountains and Silesia-Cracow successions (Figs. 7–12), including the first reliable, diagenetically unaltered data of $\delta^{13}\text{C}_{\text{org}}$ and $\delta^{18}\text{O}$ in biogenic apatite, refine this large biogeochemical perturbation on the south Laurussian shelf. This *punctata* Event, lasting ca. 1 Ma (see Kaufman 2006), is subdivided into two positive-to-negative excursions, encompassing four isotopic events, as presented for the Wietrznia Ie reference section (Fig. 7). The global extent of these positive $\delta^{13}\text{C}_{\text{carb}}$ shifts, the largest recorded in the Devonian, are demonstrated by similar correlative excursions reported from Lower to Middle Frasnian marine sediments of south Laurussia (Zhuravlev et al. 2006; Yans et al. in press) and South China (Xue-Ping Ma, personal communication 2006).

Comparing biostratigraphical dates and C-isotopic inorganic and organic secular patterns on a regional scale, compiled in Fig. 16, leads to the following conclusions:

- The $\delta^{13}\text{C}$ values obtained through most of the *Palmatolepis transitans* Zone show the Frasnian background values, which average ca. 1‰ (see Hallam and Wignall 1997: 20, Yans et al. in press).
- A weak incipient positive $\delta^{13}\text{C}_{\text{carb}}$ (only) excursion is recognized across the *Ancyrodella africana*-*A. pramosica* level exclusively at Kostomłoty and Wietrznia (up to 1.4‰ above the background level; event I, see Figs. 7 and 10), in somewhat disparity with the larger shift documented in the Belgian successions (see Racki et al. 2004).
- The $\delta^{13}\text{C}$ values decrease by ca. 2% (with $\delta^{13}\text{C}_{\text{carb}}$ as low as nearly -1‰ at Wietrznia Id) primarily in the latest part of the *Pa. transitans* Zone (step II), with the main exception of the condensed Kowala section.
- An abrupt positive $\delta^{13}\text{C}$ shift (step III) of about 2‰ (Kostomłoty) to 5‰ (Wietrznia Id) starts across the broad *Pa. transitans*-*Pa. punctata* transition at all sections. Nevertheless, the stratigraphically expanded isotopic record at Kostomłoty indicates the Early Frasnian (*Pa. transitans*) initial onset of this step (Fig. 10), and this trend is confirmed at Kowala (Fig. 11) and generally corresponds to the Ardenne C-isotopic pattern (Yans et al. in press). The data suggest a fragmentary stratigraphic record, mostly due to sediment starvation, in the other successions studied (Figs. 16, 17). The $\delta^{13}\text{C}_{\text{carb}}$ highstand values, typically between 3 and 4‰, continue through most of the *Pa. punctata* Zone, with the peak of 4.5‰ especially well documented in bulk micrite samples from Kowala.
- This isotopic “plateau” is followed in the latest part of the *Pa. punctata* Zone (*A. gigas* form 2 level) by a return to negative $\delta^{13}\text{C}$ values (the ending step IV), and then to background or even positive values in the *Pa. hassi* Zone, corresponding to the cycle 7 of Yans et al. (in press).

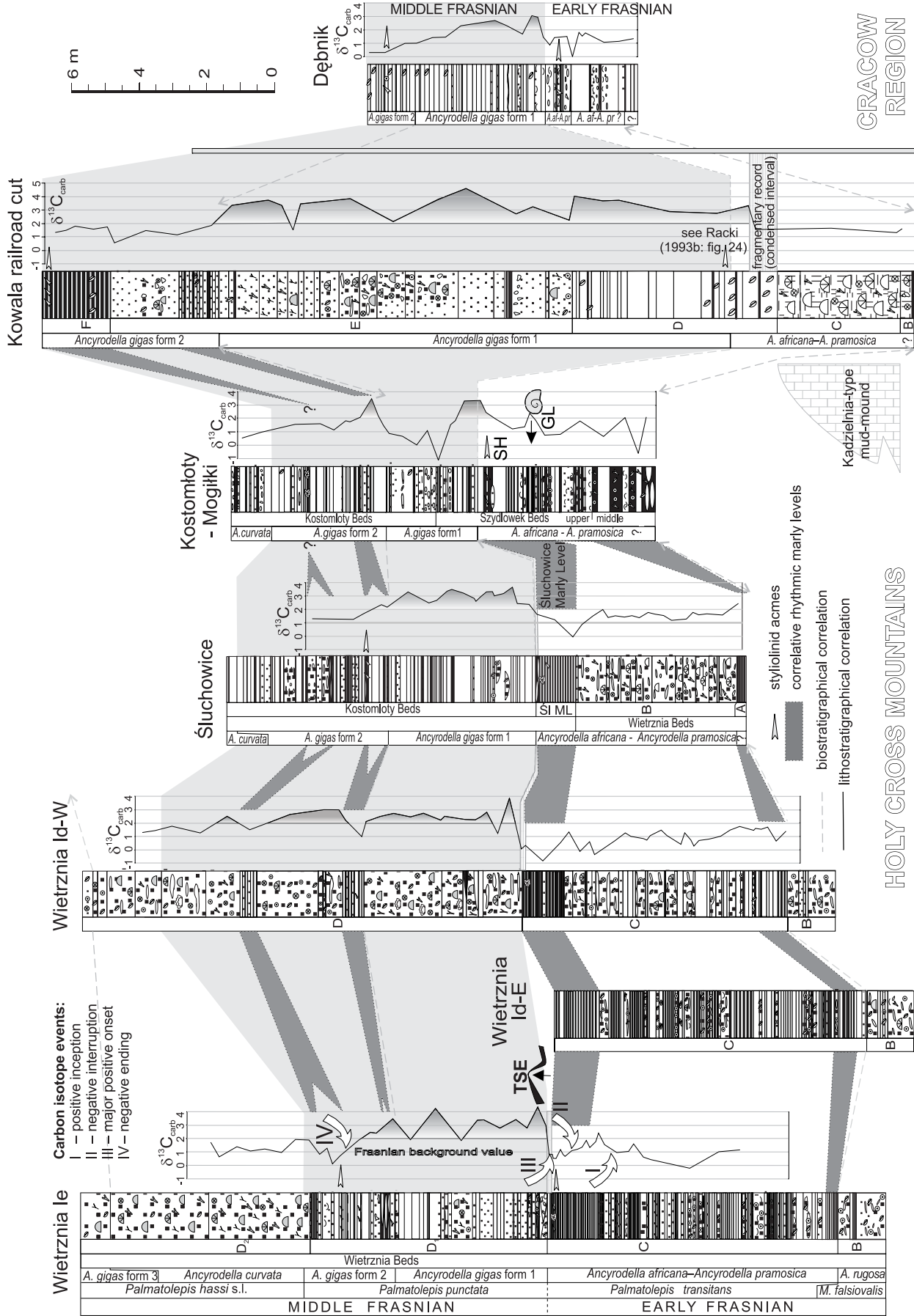


Fig. 16. Bio-, litho- and chemocorrelation of Frasnian sections under study (for detailed successions see Figs. 7–12), supplemented by literature data (e.g., Racki and Bultynck 1993; Racki et al. 2004). The major geochemical anomaly interval in the *Palmatolepis punctata* Zone is marked as a grey interval. Abbreviations: GL, Goniatite Level, see Racki et al. (2004); SH, Styliolina Horizon, see Racki et al. (2004); TSE, tectono-seismic event; A., Ancyrodella; A. afri.-A. pr., *Ancyrodella africana*–*A. primosica* conodont level; M., *Mesonatis*; Pa., *Palmatolepis*.

Consequently, both bio- and chemocorrelation tools are critical in dating of the sections under study, and when paired with lithological markers of deepening pulses (Figs. 16–18), resulted in a very precise regional stratigraphical scheme for this Frasnian interval throughout the South Polish shelf. In addition, such complicating sedimentary effects as intraformational erosion, stratigraphic condensation and hiatuses and/or diagenetic overprint, which are often formed during rapid sea-level rise, are more conclusively revealed (Figs. 7–11).

Chemostratigraphic re-evaluation of the Kadzielnia mud-mound age.—For the ecostratigraphical consideration of the E–MF interval in the southern Holy Cross Mountains (and the whole Małopolska Block; Sobstel 2003), key significance is linked with the unique facies of the mid-slope Kadzielnia mud-mounds (= Kadzielnia Limestone Member of Narkiewicz et al. 1990), being a site of extraordinarily rich benthic life (see summary in Szulczewski and Racki 1981 and Racki 1993b). However, the main constraint is the uncertain temporal relations between the major C-isotope anomaly and the extinction of the biohermal biota. Until now, conodont dating of smaller stromatoporoid-alveolitid buildups (few meters thick), known from the southern periphery of the Dyminy Reef (Szulczewski and Racki 1981), has clearly indicated that their growth was stopped by the IIc eustatic sea-level rise (Racki 1993b), and, as confirmed by the present work, this biohermal facies is marked by $\delta^{13}\text{C}$ depletion and correlates with the pre-perturbation (*Palmatolepis transitans*) phase only at Kowala (Fig. 11).

However, the age of the large (ca. 50 m thick) buildup at the type locality on the northern slope of the Dyminy Reef, bounded mostly by an erosional unconformity, remained unclearly defined because the conodont-poor biolithites were assigned to a broad *Pa. transitans*–*Pa. punctata* (?even *Pa. hassi*) zonal interval (see summary in Szulczewski and Racki 1981; Narkiewicz et al. 1990). Thus, a possibility of diachronous and prolonged development cannot be excluded, especially considering that a similar coral bindstone facies is also known at Wietrzna, probably in the basal Frasnian Wietrzna Beds (Szulczewski and Racki 1981).

The large-scale changes of $\delta^{13}\text{C}_{\text{carb}}$ across the E–MF transition offer another possibility to re-consider this dating dilemma from the chemostratigraphical viewpoint. All five brachiopod calcite samples taken along the mound section at Kadzielnia display $\delta^{13}\text{C}_{\text{carb}}$ values between 1.39‰ and 2.47‰ (Yans et al. in press), and accordingly a signature of the major positive C-isotopic excursion is not detected in the buildup. Thus, it is reasonable to assume that the major growth phase of the Kadzielnia mud-mounds on both slopes of the Dyminy Reef was limited to the *Pa. transitans* Zone, i.e., it did not continue longer than the duration of the two initial steps of the major E–MF biogeochemical disturbance (Fig. 16). In addition, the refined correlation and conodont biofacies suggest that the lateral equivalents of this bioherm include not only coral biostromes with shaly intercalations (see Szulczewski and

Racki 1981), but also the non-fossiliferous Śluchowice Marly Level and brachiopod-bearing clayey-nodular set at Jaźwica (see Racki 1993b: figs. 23B and 24), and the muddy coral biostromes within the Sitkówka lagoonal succession (Racki 1993b: fig. 36; see Fig. 17).

Wietrzna section as a potential substage stratotype.—Sections that contain an unbroken conodont faunal sequence as well as a good representation of other taxonomic groups and geochemical, MS (magnetosusceptibility), and stratigraphical marker beds should be considered by the SDS for reference and stratotype designation.

The requirements are easily met by the inactive Wietrzna quarry reference succession in Kielce, Holy Cross Mountains, which is preserved as the Zbigniew Rubinowski Reserve (Figs. 5C, D, 7, 8), due to the current high-resolution conodont and isotopic study, supplemented by paleontological, geochemical, sedimentological and MS works (Baliiński 2006; Głuchowski et al. 2006; Sobstel et al. 2006; Vierek in press). In fact, this readily accessible outcrop with a wide range of auxiliary sections was previously proposed by G. Racki in an e-mail submission to the SDS as an auxiliary stratotype succession for neritic facies marked by abundant benthic assemblages (see <http://www.geneseo.edu/~frasnian/27July2000R.htm>), in addition to the deeper water Chut River locality in southern Timan, Russia (Becker et al. 2001).

The Wietrzna section perfectly records the abrupt positive isotopic shift of the *punctata* Event and MS value drop across the substage boundary, as well as an excellent example of the ancyrodellid evolutionary sequence (as noted for older levels by Racki and Bultynck 1993) with a markedly delayed entry of the index palmatolepids, a typical case in reef complexes worldwide. The fossiliferous, essentially non-condensed succession allows comprehensive correlations between the main isotopic trends and conodont and benthic faunal changes. Diverse vertebrate remains are also abundantly represented in detrital lithologies (see Liszkowski and Racki 1993; Makowska 2001), as well as stylolinids in some marly-micritic intercalations. Unfortunately, thermal maturation is too high for refined palynofacies study (Paweł Filipiak, personal communication 2006). On a regional scale, the deeper water Kostomłoty sections, marked by a more extended record and palmatolepid-rich faunas with ammonoid contribution, offer significant supplementary biostratigraphical data (Racki et al. 2004; Jagt-Yazykova et al. 2006; Sobstel et al. 2006).

Introduction to ecosystem stratigraphy

The eustatic framework of the Late Devonian sedimentation on the Laurussian carbonate shelf, being a prerequisite for the recognition of biotic events, has been established using advanced biostratigraphical-facies studies. It was discussed by Narkiewicz (1988) and Racki (1993b, 1997) for the South

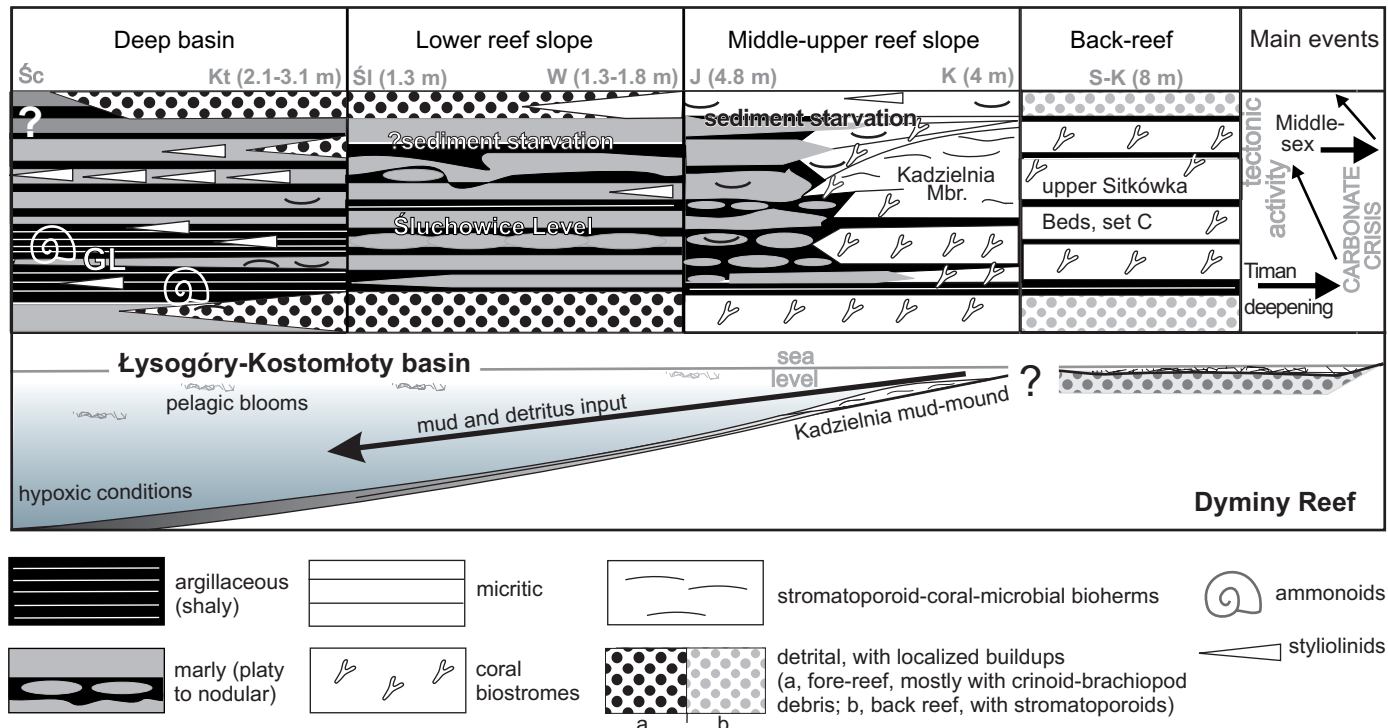


Fig. 17. Lateral facies and thickness variation by the transient reef retreat interval just prior to the Early–Middle Frasnian boundary in the Holy Cross Mountains, related to Timan and Middlesex transgressive events and subsequent eustatic sea-level falls (arrowed), and regional synsedimentary tectonism, against a simplified reconstruction of the depositional environments, principally along the northern ramp-style slope of the Dyminy Reef marked by finally accelerated mud-mound growth (complementary data from Szulczewski and Racki 1981; Racki 1993b; Racki et al. 2004; Krawczyński et al. 2006; Sobstel et al. 2006). For localities see Fig. 2 (J, Jaźwica; K, Kowala; Kt, Kostomłoty; S-K, Sitkówka-Kowala; Šc, Ściegny; Śl, Śluchowice; W, Wietrzna); GL, Goniatite Level.

Polish shelf, and refined by the conodont biofacies analysis of Sobstel et al. (2006; Figs. 17, 18). There is an overall accordance of the recognized events with the Euramerican sea-level curve of Johnson et al. (1985), even if the E–MF global eustasy pattern is far more complex, as revealed previously by Walliser (in Weddige 1998), Gouwy and Bultynck (2000), Whalen et al. (2000), Uyeno and Wendte (2005) and MacNeil and Jones (2006), among others.

In eastern North America, the Middlesex Shale marks the base of the Sonyea Group and this transgressive pulse has been used to define TR Cycle IIc of Johnson et al. (1985). The eustatic pulse has been noted in other regions of North America and in Timan, Australia, Morocco, and South China, and a spread of hypoxia associated with this TR cycle is best exemplified by the argillaceous and cherty, bituminous Domanik facies (see summary in Becker and House 1998 and Becker et al. 2001). There is still uncertainty about the age of the basal Middlesex Shale, and thus the IIc deepening pulse, in terms of conodont biostratigraphy. Over et al. (2003) only approximately linked this global event with the basal *Pa. punctata* (MN 5) Zone, because this crucial level is in fact marked by appearance of *Ancyrodella gigas* form 1 below the index palamatolepid species.

As shown by Racki (1993b, 1997), the E–MF transition on the South Polish shelf also coincides with extensive facies changes related to intermittent sea-level rise (eustatic cycles

IIb/c and IIc), probably separated by a stillstand phase; the conodont biofacies evolution suggests strongly a more convoluted, mostly sea-level lowstand setting of the E–MF interval that was interrupted by the Timan deepening pulse (Sobstel et al. 2006; see below). Incipient drowning of the expanding Dyminy Reef (see Racki and Sobstel 2004) is recorded in rapid introduction of open-shelf regimes into the reefal domain (exemplified by the *Phlogiderhynchus* Marly Level and middle Wietrzna Beds) taken as the base of the Early Frasnian IIb/c transgressive pulse in the crudely timed *A. rugosa* to *A. africana*–*A. pramosica* (= MN3 to MN4; Over et al. 2003) transition interval. However, its eustatic nature is uncertain because the global Genundewa Event is placed recently in a distinctly older interval (MN2 or *A. rotundiloba* level; House 2002, House and Gradstein 2004). On the other hand, Day (1996) linked his IIB-2 deepening event in the North American interior basin with MN3 zone (see also cycle IIB-3 of Day and Whalen 2003), and thus the record of the Genundewa Event may be highly diachronous and biased by epeirogenic effects.

The refined conodont-based dating of the Holy Cross successions indicates that the regional record of the major IIc eustatic rise across the E–MF passage interval is biased by synsedimentary tectonics (Figs. 16–18; see below), also recognizable in conodont biofacies evolution (Sobstel et al. 2006). Decreased terrigenous input and increased productiv-

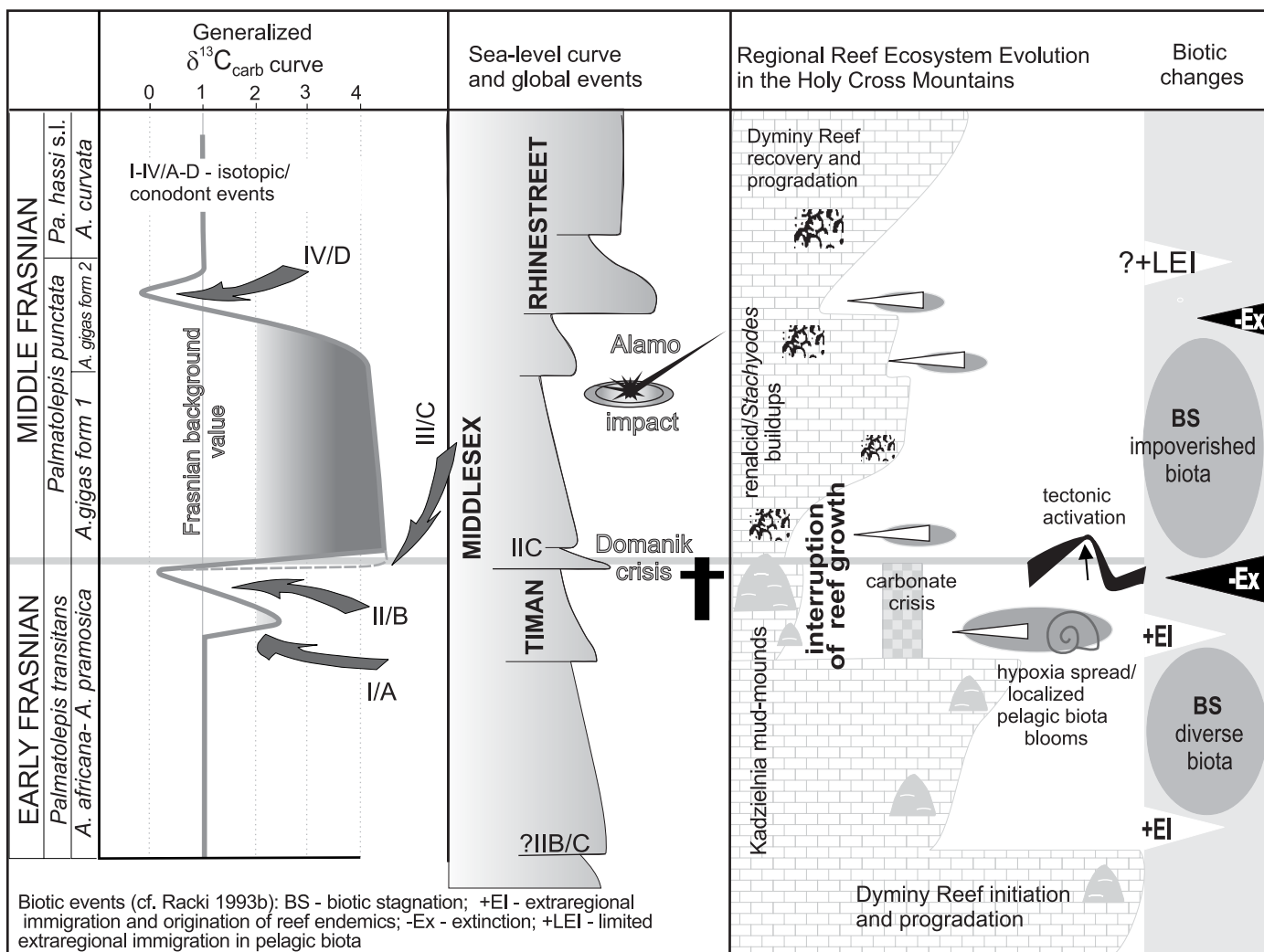


Fig. 18. Early to Middle Frasnian ecosystem stratigraphy of the Holy Cross Mountains, plotted against global biotic and eustatic events and generalized $\delta^{13}\text{C}_{\text{carb}}$ events based on the Wietrzna reference section, but shown with possible error in the record of major excursion onset (see also Racki et al. 2004: fig. 12); the regional geobiological history follows mainly conodont diversity dynamics and frequency pattern (Sobstel et al. 2006).

ity and anoxia occurring in the photic zone are a signature of the Middlesex Event (Leszek Marynowski and Jerzy Nawrocki, personal communications 2006), but the phenomena developed with a complicated temporal pattern in particular localities. Furthermore, two younger deepenings, without associated enhanced productivity/hypoxia, were established in stylolinid-rich benthos-poor marly lithofacies in the late *Palmatolepis punctata* Zone (*Ancyrodella gigas* form 2 fauna), exemplified particularly by set F at Kowala in the *Pa. punctata*-*Pa. hassi* transition (Fig. 16). This facies development, corresponding already to initiation of the multiphase Rhinestreet Event (House 2002), is known from more southern parts of the carbonate shelf as well (Narkiewicz 1978; Sobstel 2003; Fig. 18).

The late *Pa. transitans*-early *Pa. punctata* time interval is not considered as a time of significant faunal turnover (see Yans et al. in press). Moreover, the *Pa. punctata* Zone is regarded as representing optimum environmental conditions

for development of the marine biota, at least for conodonts and phytoplankton (Zhuravlev et al. 2006; Paweł Filipiak, personal communication 2006). However, only the stress-resistant conodonts, which went through the E-MF perturbational interval, bloomed during the long-term stabilization phase in the early Middle Frasnian. The E-MF the conodont biodiversity depletion has definitely a stepwise nature, alongside with biogeochemical cycling changes, as refined by Sobstel et al. (2006; Fig. 18), and may be partly correlated with the obviously more fragmentary recognized macrofaunal changes.

During the late part of the *Pa. transitans* zonal timespan a gradual decline of Early Frasnian reef-related biota occurred. In fact, the transgressive Timan Event (Figs. 17, 18), marked by episodic blooms of unique goniatite- and stylolinid-rich associations in the northern Kostomłoty-Łysogóry basin during the *A. africana*-*A. pramosica* timespan (Dzik 2002; Racki et al. 2004; Jagt-Yazykova et al. 2006), was certainly

involved as well in the onset of the prominent Dyminy Reef retreat and its backstepping style of growth. Synchronously, there is an increase in the abundance of *Icriodus* from barely a few percent to as much as 80%. This faunal dynamic trend is interpreted as an opportunistic infilling of the abandoned niche triggered by gradual but punctuated deepening, partial reef flooding and thus narrowing of the natural *Ancyrodella* habitat. The initiation of this turnover of conodont communities coincides with the short-term positive carbon isotope excursion (inception event I, Racki et al. 2004; Fig. 16). The most spectacular signature of carbonate factory perturbation is the demise of very diverse, mostly endemic biota of the mid-slope Kadzielnia mud-mounds, best evidenced in distinctive brachiopod (*Parapugnax brecciae-Fitzroyella alata*) and gastropod (*Euryzone kielcensis* and *Grabinopsis guerichi*) associations, although the most opportunistic species survived this environmental stress (Szulczeński and Racki 1981; Krawczyński 2002, 2006). Several other reef-dwelling groups (e.g., ostracods, echinoderms) await more strict examination in this context. Among the reef-builders, Wrzołek (1988, 1993) characterized rugose corals from the broad E–MF transition as distinguished by the low diversity and relatively endemic *Macgea–Thamnophyllum–Hexagonaria hexagona* assemblage.

The conodont biofacies data indicate that the late *Palmatolepis transitans* and late *Pa. punctata* zonal timespans were marked by significant sea-level fluctuations. The late *Pa. transitans* biofacies provides evidence for two rapid and short sea-level rises followed by noticeable eustatic drops. Similarly, the late *Pa. punctata* Zone interval witnessed a large-scale T-R cycle. Change in the global sea level, as indicated by change in conodont assemblage composition, should constitute an additional and valuable tool for a high-resolution stratigraphic correlation of this time interval.

On the other hand, this two-step drowning trend, corresponding to the Timan and Middlesex global hypoxic-transgressive events (House 2002; House and Gradstein 2004), was paired with limited intra-regional immigration of the benthic faunas with distinct Łysogóry-Kostomłoty affinities. This biotic pattern is well expressed in the diverse rhynchonellid-dominated bottom-level faunas (*Phlogiderhynchus polonicus* and *Flabellulirostrum–Coeloterorhynchus* assemblages; Racki 1993a; Racki et al. 1993; see more details in Baliński 2006).

The prominent but diachronous drop in frequency and biodiversity across the E–MF boundary is manifested not only in sessile and vagile benthos (brachiopods, crinoids, gastropods) and overall carbonate production, but also in nektonic conodonts (Baliński 2006; Głuchowski et al. 2006; Krawczyński 2006; Sobstel et al. 2006). This diversity drop was reinforced by a general absence of biogeographical newcomers in the Holy Cross area (with the exception of Russian conodont newcomers during the initial Rhinestreet transgression; Sobstel et al. 2006). Surprisingly, this isolation is strongly weakened in the Dębnik basin, at least among brachiopods

(*Cyrtospirifer bisellatus* and *Plionptycherhynchus cracoviensis* assemblages) and conodonts (Baliński 1979, 2006; Sobstel et al. 2006). The early Middle Frasnian stagnation/impoverishment phase resembles the similar ecosystem state of the narrowed Middle to Late Devonian transition (Racki 1993b), also marked by a large scale perturbation in carbon cycling in this part of Laurussian shelf (Yans et al. in press). However, some Givetian relics went extinct during the Middle Frasnian high-stress interval, as shown by low-diversity gastropods of the *Straparollus laevis* Assemblage (Krawczyński 2006). This impoverished biotic mode is certainly reversed in the Late Frasnian reef-cap phase (e.g., Wrzołek 1988, 1993; Racki 1993b; Krawczyński 2002), even if the preceding moderate reef recovery phase in the *Pa. hassi–Pa. jamiae* interval, evidenced in renalcid-dominated buildups in the Dyminy reef-core facies (see also Godefroid and Racki 1990), remains poorly known.

Regional tectonic factors.—Different scale environmental agents and feedbacks obviously shaped the biotic pattern outlined above. Among local or at most regional controls across the E–MF transition, the most obvious refer to synsedimentary early Variscan tectonics, or block tilting (e.g., Szulczeński 1971, 1989; Racki and Narkiewicz 2000; Lamarche et al. 2003). These factors are responsible for rapidly increasing downslope mud and debris input from reef shoals, recorded in coarse-grained conglomerate and breccia layers interrupting quiet-water marly “background” deposition, even in the distal Kostomłoty area. The combination of large-scale deepening pulse and counterbalancing uplifting events is clearly recorded in mixed conodont biofacies (Sobstel et al. 2006). Block movements are recorded at the Wietrznia sections by rapid lateral thickness and fore-reef facies changes (see Szulczeński 1989; Dzik 2002), as well as by an abrupt increase of carbonate mud and fine detritus depositional rates that overwhelmed the effects of increased terrigenous supply (evident from Sr isotopic and MS data; Eleanor John and Jerzy Nawrocki, personal communications 2006). In addition, wedge-shaped lithologies in the basal part of the *Pa. punctata* Zone are a signature of mass movements (?sliding) probably promoted by faulting and/or seismic shocks.

Hence, the tectonic factors certainly modified benthic habitats in a local scale, influencing morphological differentiation and thus circulation patterns particularly over the northern slope of Dyminy Reef. More importantly, this activity was responsible for masking the IIc deepening pulse in most of the Holy Cross localities studied (with the exception of Kowala) and for episodic development only of anoxia during the Middlesex sea-level rise (Fig. 18). Thus, despite the several sea-level changes implied from eustatic movements, the general facies setting of the recognized succession is relatively stable.

Regional or global biotic pattern?—The Frasnian age was characterized by a sequence of major environmental and evolutionary global perturbations, but the E–MF interval is rather poorly studied with the exception of goniatite and

conodont faunas. For example, ammonoids show serious extinction near the end of the *Palmatolepis transitans* Zone, followed in the *Pa. punctata* Zone with the Rhinestreet transgression (see summary in Becker and House 1998 and Becker et al. 2001). Among conodonts, variable turnover rates are known in ancyrodellids and mesotaxids, and the evolutionary pattern is largely replicated in faunas under study, especially in a diversity reduction broadly corresponding with the Domanik Crisis (Sobstel et al. 2006). In the Middle Frasnian, great sea-level changes of the initial Rhinestreet events and consequent environmental stress in the later *Pa. punctata* Zone are paired with successive replacement of *Mesotaxis*-dominated faunas by *Palmatolepis*-dominated faunas (Ziegler and Sandberg 2001: 340).

The succession is far more complicated within the benthic biota, as shown by Baliński (2006) for intra-regionally differentiated brachiopod assemblages in the Holy Cross area, as well as between the Holy Cross and Cracow shelf seas. Comparisons with other regions reveal a mosaic pattern of the changes in response to distinctly predominating local control, as exemplified by diverse brachiopod faunas of the Boulonnais area, France (Brice 2003), Iowa Basin (Day 1996, 1998) and South China (Ma et al. 2006). Replacement of crinoid and ostracod faunas across the E–MF boundary is also viewed by Guchowski et al. (2006) as a regional-scale only biotic phenomenon.

A more general control is recognizable among some brachiopod associations, however. The E–MF interval seems to be a time of cyrtospiriferid (and such other spiriferids as *Eleutherokomma*) expansion, and the radiation is strengthened during the Middlesex deepening pulse, best evidenced at Dębnik (Baliński 2006) and on the East European Platform (Lyashenko 1959, 1973; Zhuravlev et al. 2006). On the South China shelf, this brachiopod turnover is delayed as late as the the *Pa. punctata*–*Pa. hassi* zonal transition (Ma et al. 2006).

The *Pa. punctata* Zone transgression coincided with the demise of the F2d Arche mud-mounds in the Ardenne basin (see below), and this is a partly correlative event with the above emphasized collapse of the Kadzielnia-type biothermal biota. In broader terms, however, no more significant crises are known among reef-building biota and overall carbonate production (Copper 2002), and the Early to Middle Frasnian transition is shown as an evolutionarily quiet timespan in the global biodiversity curve of Sepkoski (1996: fig. 6).

Deciphering biotic response to the global biogeochemical signal

On the whole, the *punctata* Event (*sensu* Yans et al. in press) can be related to global variations in the $\delta^{13}\text{C}$ of the dissolved inorganic carbon in the oceans over this time span that reflect evolving complex relations between land, sea and biosphere. It is difficult to separate out a single primary

source of isotope distribution. The positive excursion of $\delta^{13}\text{C}$ could be the result of primary processes such as upwelling of deeper water and/or increased photosynthesis (which first of all utilizes ^{12}C) and thereby increased surface productivity (e.g., Hallam and Wignall 1997; Joachimski et al. 2001; Racki et al. 2004). The ^{13}C enrichments are paired with exceedingly enhanced bioproductivity and organic matter burial in anoxic conditions reaching the photic zone (as evidenced by biomarkers; Leszek Marynowski, personal communication 2006), which suggests fluctuations of the chemocline during the Early to Middle Frasnian intermittent sea-level rises (Fig. 15). An extraordinary acceleration of plant-mediated chemical weathering and productivity may have resulted in progressive land-derived nutrient input, especially effective when strengthened by tectonic continental uplift, as indicated by an increasing $^{87}\text{Sr}/^{86}\text{Sr}$ trend and by lowering MS values, together with synsedimentary block movements in the Holy Cross domain seen as a regional signature of more widespread tectonic activation (Jerzy Nawrocki, personal communication 2006). This is assumed to be a crucial control on the generally elevated marine bioproductivity in a generally stabilized greenhouse setting (ca. 25–28°C), even if a weak cooling trend is deduced from rising $\delta^{18}\text{O}$ values in biogenic apatites. In addition to a suddenly reduced burial rate of organic carbon, massive discharge of oceanic methane hydrate reservoirs could also promote the $\delta^{13}\text{C}$ depletion episodes in the E–MF transition owing to seismic or volcanic activity and/or several bolide strikes (see discussion in Yans et al. in press).

The trends in the conodont dynamics, mortality, and diversity conclusively confirm that the biotic turnovers across the E–MF boundary correlate directly with the main $\delta^{13}\text{C}$ excursions and related trophic conditions (Sobstel et al. 2006). The first conodont decline is contemporaneous with a transient reef biota crisis and dropping carbonate production. A gradual reduction in diversity of the Early Frasnian *Ancyrodella* fauna coincides with the weak positive and subsequent larger negative $\delta^{13}\text{C}$ anomaly. The later part of this interval is related to development of *Belodella*-rich biofacies suggesting expansive growth of mud-mounds in nearby areas (Fig. 17). In fact, the Śluchowice Marly Level, which passes laterally into the Kadzielnia mud-mounds and metre-scale coral biostromes, exemplifies the distinctive depositional and ecological character of the latest Early Frasnian interval under study. This system tract was developed most intensively during a weakened carbonate factory, probably on a gentle, ramp-type slope (Szulczeński and Racki 1981), where mud-mounds existed coevally with somewhat starved muddy-calcareous sedimentation (Fig. 17), together with conjectural vigorous keep-up reef segments in the central Kielce subregion (Racki 1993b). In the Ardenne type area, a similar facies association is usually associated with the IIc sea-level rise (Johnson et al. 1985; Becker and House 1998), but the far thicker Arche Reefs started in the coeval Early Frasnian interval in the lowstand setting (see Godefroid and Racki 1990; Gouwy and Bultynck 2000; Da Silva and Boul-

vain 2004; see also Canadian ramp-situated reef examples in MacNeil et al. 2006).

The long-term positive $\delta^{13}\text{C}$ excursion in the *Palmatolepis punctata* Zone is reflected in biofacies unification but, on the other hand, it is distinguished by an increase in the size of conodont elements in probably eutrophicated and partly anoxic regimes. The late *Pa. punctata* Zone negative carbon isotope anomaly is synchronous with the second large-scale biofacies remodelling, including mesotaxid demise, as well as with a reduction of conodont size and an increase of juvenile mortality. A stabilization of the carbon isotope curve and its return to normal background values at the start of the early *Pa. hassi* Zone coincide with conodont biofacies diversification and return to the occurrence of reef-related, ancyrodellid biofacies.

Consequently, together with intra-regional migrations promoted by intermittent deepening pulses on the South Polish shelf, the large-scale ecosystem changes are recognizable during a time interval of a major biogeochemical perturbation in the broad E–MF transition. The main factors responsible for such a carbonate-shelf ecosystem response are seen in fluctuating primary production levels within a generally uniform environmental setting, even if several other destructive agents (anoxia, cooling) were probably involved as well (see also summary in Racki et al. 2004). Thus, the rising eutrophication during positive carbon isotopic shifts influenced biotic components that were more sensitive to nutrification, such as some reef builders, shelly benthos and possibly conodonts. However, major development of the Kadzielnia mound-bearing ramp was tied to the inception stage of the major C-isotopic anomaly during the transient carbonate crisis (event I; Figs. 17, 18). The collapse of this unique reef biota was otherwise probably controlled by onset of the major positive excursion.

According to the results of Pérez-Huerta and Sheldon (2006), spiriferids and other spire-bearing groups were the most thriving brachiopods in high-nutrient habitats because of their lophophore's ability to generate strong inhalant unidirectional currents in the restricted areas around the shell. Thus, the successful colonization of some carbonate shelves by cyrtospiriferids during the $\delta^{13}\text{C}$ highstand of the *punctata* Event may have been promoted by the suitable nutrification phenomena (see also conodont record in Zhuravlev et al. 2006), if such other limiting factors as benthic hypoxia were neglected.

Conclusions

Conodont associations from the *Palmatolepis transitans*–*Palmatolepis punctata* zonal boundary beds are dominated by the shallow-water taxa of polygnathid and/or ancyrodellid biofacies in South Polish epicontinental successions, and first appearances of index palmatolepid species were delayed due to facies control of the pelagic biofacies during intermittent drowning of the carbonate shelf (Racki and

Bultynck 1993; Sobstel et al. 2006). Thus, identification of the key zonal boundary is based mainly on species of *Ancyrodella*, and five distinctive ancyrodellid levels occur in the succession across the E–MF interval, enabling refined correlation of the sections studied, especially when paired with chemostratigraphic proxies (Fig. 16).

Prominent conodont biofacies shifts coincided with the eustatic deepening correlated with the Timan, Middlesex and early Rhinestreet events (Sobstel et al. 2006). Trends in the conodont dynamics, mortality and diversity, partly replicated by benthic biota, indicate that the faunal turnovers correlate also with the main $\delta^{13}\text{C}$ excursions and related trophic conditions. The E–MF transitional interval, marked by short-term sea-level fluctuations, is distinguished by a change from relatively diversified biofacies to more homogenous, mostly impoverished faunas. The latter change is a biotic response to the beginning of the prolonged (ca. 0.5 Ma) positive $\delta^{13}\text{C}$ anomaly, probably paired with unsteady eutrophicated and partly anoxic regimes. The late *Pa. punctata* Zone negative carbon isotope anomaly is synchronous with the second large-scale pelagic biofacies remodelling, including mesotaxid extinction, as well as in reduction of conodont size and increased juvenile mortality. A stabilization of carbon cycling and the return to its normal background values at the start of the early *Pa. hassi* Zone coincide with conodont biofacies diversification and recovery of reef-related biofacies.

With the exception of the collapsed endemic Kadzielnia-type mud-mound biota and a moderate biodiversity depletion due to overall ecosystem stagnation, no significant extinction events can be proved, even if the large-scale changes in carbon cycling in the E–MF timespan are of higher amplitude than the biogeochemical turnovers during the Frasnian–Famennian mass extinction. Thus, this regional biotic succession confirms that the large-scale *punctata* Isotopic Event is correlated neither with catastrophic environmental nor with any radical biotic changes (Yans et al. in press). Notably, these recorded shifts in the $\delta^{13}\text{C}$ are of higher-amplitude than the celebrated biogeochemical turnovers related to the F–F mass extinction (below 3‰), but not connected with a dramatic breakdown of carbonate production.

Acknowledgements

This work has been supported by the State Committee for Scientific Research (KBN grant 3 P04D 040 22 to G. Racki). We are deeply indebted to journal referees Jared R. Morrow (San Diego State University, USA) and Gilbert Klapper (Glencoe, Illinois, USA) for their careful examination and stimulative comments on an earlier version of the manuscript. We thank Maria Racka, Aleksandra Vierek, Waldemar Bardziński, Marcin Lewandowski, and Anna Witek (all from the University of Silesia, Sosnowiec, Poland), for extensive help in field and technical works, to Tomasz Wrzolek (University of Silesia, Sosnowiec, Poland) for linguistic corrections and to Pierre Bultynck (Royal Belgian Institute of Natural Sciences, Brussels, Belgium) for conodont consultations.

References

- Baliński, A. 1979. Brachiopods and conodonts from the Frasnian of the Dębnik anticline, Southern Poland. *Palaeontologia Polonica* 39: 4–95.
- Baliński, A. 1995. Brachiopods and conodont biostratigraphy of the Famennian from the Dębnik anticline, southern Poland. *Palaeontologia Polonica* 54: 1–85.
- Baliński, A. 2006. Brachiopods and their response to the Early–Middle Frasnian biogeochemical perturbations on the South Polish carbonate shelf. *Acta Palaeontologica Polonica* 51: 647–678.
- Becker, R.T. and House, M.R. 1998. Proposals for an international substage subdivision of the Frasnian. *SDS Newsletter* 15: 17–22. <http://sds.uta.edu/Newsletter15/nl15body.htm>.
- Becker, R.T., Menner, V.V., Ovnatanova, N.S., Kuzmin, A., and House, M.R. 2001. A potential Middle Frasnian Stratotype Section at Chut River (Southern Timan, Russia)—a preliminary account. *SDS Newsletter* 18: 45–51. <http://sds.uta.edu/sds18/page0045.htm>.
- Bednarczyk, J. 1990. Geneza struktur gruzłowych w wapieniach dębnickich (żywot/frań) w świetle badań sedymentologicznych i analizy zawartości izotopów stałych węgla i tlenu. *Przegląd Geologiczny* 38: 206–209.
- Bednarczyk, J., Hoffmann, M., and Paszkowski, M. 1997. The Upper Devonian cryptomicrobial-algal-stromatoporoid buildups from the Holy Cross Mountains, Poland. Stop 10. Kadzielnia, abandoned quarry. The Holy Cross Mountains. In: *3rd IFAA Regional Symposium & IGCP 380 International Meeting, Guidebook*, 3–7, 47–48. Institute of Geological Sciences, Jagiellonian University, Cracow.
- Borcuch, E. 2006. *Górnodewońskie konodonty z Góra Świętokrzyskich – aspekty paleoekologii i biostratygrafii na przykładzie profili Kostomłotów i Kowali*. 38 pp. Unpublished M.Sc. thesis, University of Silesia, Sosnowiec.
- Bultynck, P., Helsen, S., and Hayduckiewich, J. 1998. Conodont succession and biofacies in upper Frasnian formation (Devonian) from the southern and central parts of the Dinant Synclinorium (Belgium) (Timing of facies shifting and correlation with late Frasnian events). *Bulletin de l'Institut royal des Sciences naturelles de Belgique, Sciences de la Terre* 68: 25–75.
- Brice, D. 2003. Brachiopod associations in the Devonian of Ferques (Boulonnais, France). Relations to palaeoenvironments and global eustatic curves. *Bulletin of Geosciences* 78: 405–417.
- Copper, P. 2002. Silurian and Devonian reefs: 80 million years of greenhouse between two ice ages. In: W. Kiessling, E. Flügel, and J. Golonka (eds.), *Phanerozoic Reef Patterns. SEPM Special Publication* 72: 181–238.
- Da Silva, A.C. and Boulvain, F. 2004. From palaeosols to carbonate mounds: facies and environments of the middle Frasnian platform in Belgium. *Geological Quarterly* 48: 253–266.
- Dadlez, R. 2001. Holy Cross Mts. area—crustal structure, geophysical data and general geology. *Geological Quarterly* 45: 99–106.
- Dadlez, R., Kowalczewski, Z., and Znosko, J. 1994. Some key problems of the pre-Permian tectonics of Poland. *Geological Quarterly* 38: 169–190.
- Day, J. 1996. Faunal signatures of Middle–Upper Devonian depositional sequences and sea-level fluctuations in the Iowa Basin: U.S. Midcontinent. In: B.J. Witzke, G.A. Ludvigson, and J. Day (eds.), *Paleozoic Sequence Stratigraphy: Views from the North American Craton. Geological Society of America Special Paper* 306: 277–300.
- Day, J. 1998. Distribution of latest Givetian–Frasnian Atypida (Brachiopoda) in central and western North America. *Acta Palaeontologica Polonica* 43: 205–240.
- Day, J. and Whalen, M.T. 2003. Western Laurussian record of regional and global Middle–Late Devonian sea level changes and bioevents: Alberta Rocky Mountains. *Geological Society of America Abstracts with Programs* 35 (6): 208.
- Dzik, J. 2002. Emergence and collapse of the Frasnian conodont and ammonoid communities in the Holy Cross Mountains, Poland. *Acta Palaeontologica Polonica* 47: 565–650.
- Gluchowski, E., Olempska, E., and Casier J.C. 2006. Crinoid and ostracod succession within the Early–Middle Frasnian interval in the Wietrzna quarry, Holy Cross Mountains, Poland. *Acta Palaeontologica Polonica* 51: 695–706.
- Godefroid, J. and Racki, G. 1990. Frasnian gypidulid brachiopods from the Holy Cross Mountains (Poland). Comparative stratigraphic analysis with the Dinant Synclinorium (Belgium). *Bulletin de l'Institut royal des Sciences naturelles de Belgique, Sciences de la Terre* 60: 43–74.
- Gouwy, S. and Bultynck, P. 2000. Graphic correlation of Frasnian sections (Upper Devonian) in the Ardennes, Belgium. *Bulletin de l'Institut royal des Sciences naturelles de Belgique, Sciences de la Terre* 70: 25–52.
- Hallam, A. and Wignall, P. 1997. *Mass Extinctions and Their Aftermath*. 320 pp. Oxford University Press, Oxford.
- House, M.R. 2002. Strength, timing, setting and cause of mid-Palaeozoic extinctions. *Palaeogeography, Palaeoclimatology, Palaeoecology* 181: 5–25.
- House, M.R. and Gradstein, F.M. 2004. The Devonian Period. In: F. Gradstein, J., Ogg, and A. Smith (eds.), *A Geologic Time Scale 2004*, 202–221. Cambridge University Press, Cambridge.
- Jagt-Yazykova, E., Krawczyński, W., and Rakociński, M. 2006. Molluscs from the Early Frasnian Goniatite Level at Kostomłoty in the Holy Cross Mountains, Poland. *Acta Palaeontologica Polonica* 51: 707–718.
- Ji, Q. and Ziegler, W. 1993. The Lali section: an excellent reference section for Upper Devonian in South China. *Courier Forschungsinstitut Senckenberg* 157: 1–183.
- Joachimski, M.M., Ostertag-Henning, C., Pancost, R.D., Strauss, H., Freeman, K.H., Littke, R., Damsté, J.S., and Racki, G. 2001. Water column anoxia, enhanced productivity and concomitant changes in $\delta^{13}\text{C}$ and $\delta^{34}\text{S}$ across the Frasnian–Famennian boundary (Kowala, Holy Cross Mountains/Poland). *Chemical Geology* 175: 109–131.
- Johnson, J.G., Klapper, G., and Sandberg, C.A. 1985. Devonian eustatic fluctuations in Euramerica. *Bulletin of the Geological Society of America* 96: 567–587.
- Kaufmann, B. 2006. Calibrating the Devonian Time Scale: A synthesis of U–Pb ID-TIMS ages and conodont stratigraphy. *Earth-Science Reviews* 76: 175–190.
- Klapper, G. 1985. Sequence in conodont genus *Ancyrodella* in the lower *asymmetricus* Zone (earliest Frasnian, Upper Devonian) of the Montagne Noire, France. *Paleontographica A* 188: 19–34.
- Klapper, G. 1988. The Montagne Noire Frasnian (Upper Devonian) conodont succession. In: N.J. McMillan, A.F. Embry, and A.F. Glass (eds.), *Devonian of the World. Canadian Society of Petroleum Geologists Memoir* 14 (3): 449–468.
- Klapper, G. 1997. Graphic correlation of Frasnian (Upper Devonian) sequences in Montagne Noire, France, and western Canada. *Geological Society of America, Special Papers* 321: 113–129.
- Klapper, G. and Becker, T. 1999. Comparison of Frasnian (Upper Devonian) conodont zonations. *Bollettino della Società Paleontologica Italiana* 37: 339–348.
- Klapper, G. and Foster, C.T. 1993. Shape analysis of Frasnian species of the Late Devonian conodont genus *Palmatolepis*. *Paleontological Society Memoir* 32, Supplement to *Journal of Paleontology* 67 (4): 1–33.
- Klapper, G. and Lane, H.R. 1985. Upper Devonian (Frasnian) conodonts of the *Polygnathus* biofacies. *Journal of Paleontology* 59: 904–951.
- Klapper, G. and Lane, H.R. 1989. Frasnian (Upper Devonian) conodont sequence at Luscar Mountain and Mount Haultain, Alberta Rocky Mountains. In: N.J. McMillan, A.F. Embry, and A.F. Glass (eds.), *Devonian of the World. Canadian Society of Petroleum Geologists Memoir* 14 (3): 469–478.
- Klapper, G., Kuzmin, A., and Ovnatanova, N. 1996. Upper Devonian conodonts from Timan–Pechora Region, Russia and correlation with a Frasnian Composite Standard. *Journal of Paleontology* 70: 131–152.
- Krawczyński, W. 2002. Frasnian gastropod synecology and bio-events in the Dyminy reef complex of the Holy Cross Mountains, Poland. *Acta Palaeontologica Polonica* 47: 267–288.

- Krawczyński, W. 2006. Gastropod succession across the Early–Middle Frasnian transition in the Holy Cross Mountains, southern Poland. *Acta Palaeontologica Polonica* 51: 679–693.
- Kuzmin, A.V. and Yatskov, S.V. 1997. Transgressive-regressive events and conodont and ammonoid assemblages in the Frasnian of the South Timan. *Courier Forschungsinstitut Senckenberg* 199: 25–36.
- Lamarche, J., Lewandowski, M., Mansy, J.L., and Szulczewski, M. 2003. Partitioning pre-, syn- and post-Variscan deformation in the Holy Cross Mts., eastern Variscan foreland. In: T. McCann and A. Saintot (eds.), Tracing Tectonic Deformation Using the Sedimentary Record. *Geological Society of London, Special Publication* 208: 159–184.
- Liszkowski, J. and Racki, G. 1993. Ichthyoliths and deepening events in the Devonian carbonate platform of the Holy Cross Mountains. *Acta Palaeontologica Polonica* 37 (for 1992): 268–275.
- Lyashenko, A.I. [Лащенко, А.И.] 1959. *Atlas brachiopod i stratigrafiâ devona Russkoj Platformy*. 451 pp. Gostontehizdat, Moskva.
- Lyashenko, A.I. [Лащенко, А.И.] 1973. *Brachiopody i stratigrafiâ niżne-frasńskich otlożeń Timana i Volgo-Uralskoj neftegazonoj prowincji*. 276 pp. Nedra, Moskva.
- Ma, X.P., Becker, R.T., Li, H., and Sun, Y.Y. 2006. Early and Middle Frasnian brachiopod faunas and turnover on the South China shelf. *Acta Palaeontologica Polonica* 51: 789–812.
- MacNeil, A.J. and Jones, B. 2006. Sequence stratigraphy of a Late Devonian ramp-situated reef system in the Western Canada Sedimentary Basin: dynamic responses to sea-level change and regressive reef development. *Sedimentology* 53: 321–359.
- Makowska, M. 2001. *Biofacje konodontowe wczesnego franu kamieniotłomu Wietrzna w Kielcach*. 32 pp. Unpublished M.Sc. thesis, University of Silesia, Sosnowiec.
- Narkiewicz, M. 1978. Stratigraphy and facies development of the Upper Devonian in the Olkusz-Zawiercie area, Southern Poland. *Acta Geologica Polonica* 28: 415–470.
- Narkiewicz, M. 1988. Turning points in sedimentary development in the Late Devonian in southern Poland. In: N.J. McMillan, A.F. Embry, and A.F. Glass (eds.), Devonian of the World. *Canadian Society of Petroleum Geologists Memoir* 14 (2): 619–636.
- Narkiewicz, M. 1996. Devonian stratigraphy and depositional environments in proximity of the Sub-Carpathian Arch: Lachowice 7 well, southern Poland. *Geological Quarterly* 40: 65–88.
- Narkiewicz, M. and Racki, G. 1984. Stratygrafia dewonu antykliny Dębnika. *Kwartalnik Geologiczny* 28: 513–546.
- Narkiewicz, M. and Racki, G. 1987. Korelacja i rozwój sedymentacji górnego dewonu między Dębnikiem a Zawierciem. *Kwartalnik Geologiczny* 31: 341–356.
- Narkiewicz, M., Racki, G., and Wrzolek, T. 1990. Litostratygrafia dewon-skiej serii stromatoporoidowo-koralowcowej w Górzach Świętokrzyskich. *Kwartalnik Geologiczny* 34: 433–456.
- Over, J.D., Hopkins, T.H., Brill, A., and Spaziani, A.L. 2003. Age of the Middlesex Shale (Upper Devonian, Frasnian) in New York State. *Courier Forschungsinstitut Senckenberg* 242: 217–223.
- Ovnatanova, N.S., Kuzmin, A.V., and Menner, V.V. 1999. The succession of Frasnian conodont assemblages in the type section of the southern Timan-Pechora province (Russia). *Bulletino della Società Paleontologica Italiana* 37: 349–360.
- Ovnatanova, N.S. and Kononova, L.I. 2001. Conodonts and Upper Devonian (Frasnian) biostratigraphy of Central Region of Russian Platform. *Courier Forschungsinstitut Senckenberg* 233: 1–115.
- Pérez-Huerta, A. and Sheldon, N.D. 2006. Pennsylvanian sea level cycles, nutrient availability and brachiopod paleoecology. *Palaeogeography, Palaeoclimatology, Palaeoecology* 230: 264–279.
- Racki, G. 1993a. Brachiopod assemblages in the Devonian Kowala Formation of the Holy Cross Mountains. *Acta Palaeontologica Polonica* 37 (for 1992): 297–357.
- Racki, G. 1993b. Evolution of the bank to reef complex in the Devonian of the Holy Cross Mountains. *Acta Palaeontologica Polonica* 37 (for 1992): 87–182.
- Racki, G. 1997. Devonian eustatic fluctuations in Poland. In: M.R. House and W. Ziegler (eds.), On Sea-level Fluctuations in the Devonian. *Courier Forschungsinstitut Senckenberg* 199: 1–12.
- Racki, G. 2005. Toward understanding Late Devonian global events; few answers, many questions. In: D.J. Over, J.R. Morrow, and P.B. Wignall (eds.), Understanding Late Devonian and Permian-Triassic Biotic and Climatic Events; Towards an Integrated Approach. *Developments in Palaeontology and Stratigraphy* 20: 5–36. Elsevier, Amsterdam.
- Racki, G. and Bultynck, P. 1993. Conodont biostratigraphy of the Middle to Upper Devonian boundary beds in the Kielce area of the Holy Cross Mountains. *Acta Geologica Polonica* 43: 1–33.
- Racki, G. and Narkiewicz, M. 2000. Tektoniczne a eustatyczne uwarunkowania rozwoju sedymentacji dewonu świętokrzyskiego. *Przegląd Geologiczny* 48: 65–76.
- Racki, G. and Sobstel, M. 2004. Very large stromatoporoid indicating Early Frasnian reef core (Holy Cross Mts., Poland). *Geological Quarterly* 48: 83–88.
- Racki, G., Głuchowski, E., and Malec, J. 1985. The Givetian to Frasnian succession at Kostomłoty in the Holy Cross Mts., and its regional significance. *Bulletin of the Polish Academy of Sciences, Earth Sciences* 33: 159–171.
- Racki, G., Makowski, I., Miklas, J., and Gawlik, S. 1993. Brachiopod biofacies in the Frasnian reef-complexes: An example from the Holy Cross Mts., Poland. *Prace Naukowe Uniwersytetu Śląskiego, Geologia* 12/13: 64–109.
- Racki, G., Piechota, A., Bond, D., and Wignall, P. 2004. Geochemical and ecological aspects of lower Frasnian pyrite-ammonoid level at Kostomłoty (Holy Cross Mountains, Poland). *Geological Quarterly* 48: 267–282.
- Sandberg, C.A., Ziegler, W., and Bultynck, P. 1989. New standard conodont zones and early *Ancyrodella* phylogeny across Middle–Upper Devonian boundary. *Courier Forschungsinstitut Senckenberg* 110: 195–230.
- Sandberg, C.A., Hasenmueller, N.R., and Rexroad, C.B. 1994. Conodont biochronology, biostratigraphy, and biofacies of Upper Devonian of New Albany Shale, Indiana. *Courier Forschungsinstitut Senckenberg* 168: 227–253.
- Sartenaer, P., Racki, G., and Szulczewski, M. 1998. The late Frasnian rhynchonellid genus *Pammegetherhynchus* (Brachiopoda) in Poland, and its relevance to the Kellwasser Crisis. *Acta Palaeontologica Polonica* 43: 379–394.
- Schätz, M., Zwing, A., Tait, J., Belka, Z., Soffel, H.C., and Bachtadse, V. 2006. Paleomagnetism of Ordovician carbonate rocks from Malopolska Massif, Holy Cross Mountains, SE Poland—magnetostratigraphic and geotectonic implications. *Earth and Planetary Science Letters* 244: 349–360.
- Sepkoski, J.J. 1996. Patterns of Phanerozoic extinction: a perspective from global data bases. In: O.H. Walliser (ed.), *Global Events and Event Stratigraphy in the Phanerozoic*, 35–51. Berlin, Springer.
- Skwarek, B. 1990. *Opracowanie mikropaleontologiczne wapieni dewońskich z kamieniotłomu Wietrzna w Kielcach*. 38 pp. Unpublished M.Sc. thesis, University of Silesia, Sosnowiec.
- Sobstel, M. 2003. *Stratygrafia dewonu południowo-zachodniej części Masywu Małopolskiego*. 119 pp. Unpublished Ph.D. thesis. University of Silesia, Sosnowiec.
- Sobstel, M., Makowska-Haftka, M., and Racki, G. 2006. Conodont ecology in the Early–Middle Frasnian transition on the South Polish carbonate shelf. *Acta Palaeontologica Polonica* 51: 719–746.
- Szulczewski, M. 1968. Slump structures and turbidites in Upper Devonian limestones of the Holy Cross Mts. *Acta Geologica Polonica* 18: 303–323.
- Szulczewski, M. 1971. Upper Devonian conodonts, stratigraphy and facies development in the Holy Cross Mts. *Acta Geologica Polonica* 21: 1–129.
- Szulczewski, M. 1981. Stratygrafia franu wzgórz kostomłockich. In: H. Żakowa (ed.), *Przewodnik 53 Zjazdu Polskiego Towarzystwa Geologicznego*, 222–225. Wydawnictwa Geologiczne, Warszawa.

- Szulczewski, M. 1989. Światowe i regionalne zdarzenia w zapisie stratygraficznym pogranicza franu z famenem Gór Świętokrzyskich. *Przegląd Geologiczny* 37: 551–557.
- Szulczewski, M. 1995. Depositional evolution of the Holy Cross Mountains in the Devonian and Carboniferous—a review. *Geological Quarterly* 39: 471–488.
- Szulczewski, M. and Racki, G. 1981. Early Frasnian bioherms in the Holy Cross Mts. *Acta Geologica Polonica* 31: 147–162.
- Uyeno, T.T. and Wendte, J.C. 2005. Conodont biostratigraphy and physical stratigraphy in two wells of the Beaverhill Lake Group, Upper Middle to Lower Upper Devonian, Central Alberta, Canada. *Geological Survey of Canada Bulletin* 369: 151–171.
- Vierek, A. (in press). Transitional reef-to-basin facies of Lower Frasnian limestones determined by microfacies analysis (Wietrzna, Holy Cross Mts., Poland). *Facies* 53.
- Walliser, O.H. 1985. Natural boundaries and Commission boundaries in the Devonian. *Courier Forschungsinstitut Senckenberg* 75: 401–408.
- Weddige, K. 1998. Devon-Korrelationstabelle, Ergänzungen 1997. *Senckenbergiana lethaea* 77: 289–326.
- Whalen, M.T., Eberli, G.P., van Buchem, F.S.P., Mountjoy, E.W., and Homewood, P.W. 2000. Bypass margins, basin-restricted wedges and platform-to-basin correlation, Upper Devonian, Canadian Rocky Mountains: implications for sequence stratigraphy of carbonate platform systems. *Journal of Sedimentary Research* 70: 913–936.
- Wrzołek, T. 1988. Tetracoral zonation of the Devonian stromatoporoid-coral limestones in the SW Holy Cross Mountains, Poland. In: N.J. McMillan, A.F. Embry, and A.F. Glass (eds.), Devonian of the World. *Canadian Society of Petroleum Geologists Memoir* 14 (3): 413–424.
- Wrzołek, T. 1993. Rugose corals from the Devonian Kowala Formation of the Holy Cross Mountains. *Acta Palaeontologica Polonica* 37 (for 1992): 217–254.
- Yans, J., Corfield, R.M., Racki, G., and Préat, A. (in press). Evidence for a major perturbation of the carbon cycle in the Middle Frasnian *punctata* conodont Zone. *Geological Magazine*.
- Zhuravlev, A.V., Sokiran, E.V., Evdokimova, I.O., Dorofeeva, L.A., Rusetskaya, G.A., and Małkowski, K. 2006. Faunal and facies changes at the Early–Middle Frasnian boundary in the north-western East European Platform. *Acta Palaeontologica Polonica* 51: 747–758.
- Ziegler, W. and Sandberg, C.A. 1990. The Late Devonian standard conodont zonation. *Courier Forschungsinstitut Senckenberg* 121: 1–115.
- Ziegler, W. and Sandberg, C.A. 2000. Utility of palmatolepids and icriodontids in recognizing Upper Devonian series, stage, and possible substage boundaries. *Courier Forschungsinstitut Senckenberg* 225: 335–347.
- Ziegler, W., Ovnatanova, N., and Kononova, L. 2000. Devonian polygnathids from the Frasnian of the Rheinisches Schiefergebirge, Germany, and the Russian Platform. *Senckenbergiana lethaea* 80: 593–645.

Appendix 1

Table 1. Composition and frequency of conodonts at Wietrznia W-Ie. Sample weight: S, below 0.5 kg, M, 0.5–1 kg, L, above 1 kg.

conodont zones		<i>Palmatolepis transitans</i>												<i>Palmatolepis punctata</i>												<i>Pa.hassi</i> s.l.							
ancyrodellid level		<i>Ancyrodella africana</i> – <i>A. pramosica</i>												<i>A. gigas</i> form 1						<i>A. gigas</i> form 2						<i>A. curvata</i>	<i>A. gigas</i> f.3						
sample weight		L	M	M	L	M	M	M	M	M	M	M	M	M	M	M	M	M	M	M	M	M	M	M	L	L	L	M					
taxa	sample number	27	28	31	48	60	66	99	105	111	135	157	160	164	168	169	171	172	179	189	195	201	206	208	209	213	225	233/1	233/2	233/3	233/4	233/5	
<i>Ancyrodella rotundiloba</i>		4	2	1	1	1	2		1						1	1			1														
<i>Ancyrodella rugosa</i>		22	6	3	90	29	5									1																	
<i>Ancyrodella alata</i>		16	3	3	9	10	8									1																	
<i>Ancyrodella triangulata</i>		4	1		5																												
<i>Ancyrodella recta</i>		3			2	1																											
<i>Ancyrodella africana</i>		2?							1?		1					1	5	1	1	1													
<i>Ancyrodella devonica</i>					1																												
<i>Ancyrodella pramosica</i>																	1																
<i>Ancyrodella gigas</i> form 1																1	1	7	3					1	1					1?			
<i>Ancyrodella gigas</i> form 2																								2	2	1							
<i>Ancyrodella lobata</i>																												1	1	1			
<i>Ancyrodella curvata</i> early form																											1	2	1		3		
<i>Ancyrodella gigas</i> form 3																																	
<i>Ancyrodella</i> sp.		16	1	6	2											1									1	1	2	1	3	1			
<i>Polygnathus pennatus</i>		5		1					1																								
<i>Polygnathus dengleri</i>		29	28	19		3			2	1																							
<i>Polygnathus dubius</i>		27		19	24	10	9				1		1	6	14	3	22	12	21	9	2	3	22	8			1						
<i>Polygnathus angustidiscus</i>		1		2	1				1	1	3			1	1			1	1								1			19			
<i>Polygnathus aequalis</i>		4		8	2	1										2?	3	16	2	18	5	6	7								2		
<i>Polygnathus decorosus</i>		8		5	2				3	1																							
<i>Polygnathus alatus</i>		4		1														3	1										1	3	2		
<i>Polygnathus</i> aff. <i>decorosus</i>																		2															
<i>Polygnathus webbi</i>				2														1		6	14	3	3	25	23	23	4	2	3	2			
<i>Polygnathus brevilamiformis</i>																													1				
<i>Polygnathus elegantulus</i>																												1	2cf	1	3	1	
<i>Polygnathus gracilis</i>																													1				
<i>Polygnathus foliatus</i>																												2		5	4		
<i>Polygnathus uchtensis</i>																												4	4	1		1	
<i>Polygnathus lordinensis</i>																												2				2	
<i>Polygnathus pacificus</i>																												5	2	3	3		
<i>Polygnathus zinaiidae</i>																												3		3			
<i>Polygnathus</i> sp.		7		11	1				1		1			1	6		5	7	2	3	2	4	2	1	4	5	2	5	5				
<i>Palmatolepis transitans</i>																		1	1														
<i>Palmatolepis punctata</i>																												1					
<i>Palmatolepis</i> sp. A																												2	1	1		3	
<i>Palmatolepis plana</i>																															1	1	
<i>Palmatolepis hassi</i> s.l.																																1?	2
<i>Palmatolepis</i> aff. <i>proversa</i>																																	1
<i>Palmatolepis</i> sp.																															1	1	3
<i>Klapperina unilabius</i>																																	
<i>Klapperina ovalis</i>		10	18	6		1	2	1									3	4	9	4	2	1	1	6	5		1						
<i>Mesotaxis falsiovalis</i>			2	1		1				1						4	2	3	1	1	3	2	1	1									
<i>Mesotaxis asymmetrica</i>									3		2	1	2		11		6	2	2	2		2											
<i>Mesotaxis costalliformis</i>															1																		
<i>Icriodus expansus</i>		4	12	7	3		1									4																1	
<i>Icriodus symmetricus</i>		14	3	4	3	16	3		2	1	1		2	11		2	4	3	10	3	2	1	6	1	1		5	1	1				
<i>Ozarkodina nanaginta</i>																																	
<i>Ozarkodina</i> sp.															1												1	2					
<i>Mehlina gradata</i>		1	2		1	5								1	1			1															
<i>Belodella</i> sp.			2	3	9	5			1	6	7			2	1			7											2	3	3		
<i>Playfordia</i> sp.			1	1	2																												
total Pa elements (and Belodella)		165	33	64	195	106	41	2	27	1	6	15	4	4	8	85	30	30	80	52	87	20	18	14	107	84	15	57	32	10	43	34	38
number of Pa elements/kg		117	33	64	139	106	41	2	27	1	6	15	4	4	8	85	30	30	80	52	87	20	18	14	107	84	15	47	23	7	31	24	38
Pb, M and S elements		118	1	171	131	158	80	0	81	5	42	48	19	5	23	87	26	47	141	56	98	8	23	18	17	75	23	56	36	11	49	30	15

Table 2. Composition and frequency of conodonts at Wietrzna W-IdE. Sample weight: S, below 0.5 kg, M, 0.5–1 kg, L, above 1 kg.

conodont zones		<i>Palmatolepis transitans</i>														
ancyrodellid level		<i>Ancyrodella africana</i> – <i>A. pramosica</i>														
sample weight	M	M	M	M	M	M	M	M	M	M	M	M	M	M	M	M
sample number	2	5	6	13	25	30	31	43	46	52	70	71	73	77	90	
taxa																
<i>Ancyrodella rotundiloba</i>	6			7		3	1		1							
<i>Ancyrodella rugosa</i>	8			8	1	32	37	2	40	3		9				
<i>Ancyrodella alata</i>	5	1	3	6	2	10	8	1	15			5				
<i>Ancyrodella triangulata</i>						3	2									
<i>Ancyrodella recta</i>						1										
<i>Ancyrodella africana</i>			2?									2				
<i>Ancyrodella sp.</i>	5	3	2	6	1	8	5	2	6			2				
<i>Polygnathus pennatus</i>	1			1		1		1			4	2				
<i>Polygnathus dubius</i>	65	12	8	109	9	15	40	1	38	1	66	28	1			
<i>Polygnathus dengleri</i>	2		1	4	1	6	29	1				1				
<i>Polygnathus pollocki</i>	13	4		4												
<i>Polygnathus foliatus</i>	3					1										
<i>Polygnathus angustidiscus</i>	2			1		2		1			3	9				
<i>Polygnathus xylus</i>	2	2														
<i>Polygnathus aequalis</i>		1		3		2	3				3	1				
<i>Polygnathus decorosus</i>	6?										1	3	1			
<i>Polygnathus robustus</i>											2	2				
<i>Polygnathus aff. lingulatus</i>											2	1				
<i>Polygnathus webbi</i>											1					
<i>Polygnathus sp.</i>	12	10	10	1		1					1	5	1			
<i>Mesotaxis falsiovalis</i>	3	1		62	11	10		3	6	1	1	1				
<i>Mesotaxis asymmetrica</i>											5	5				
<i>Mesotaxis bogoslovskyi</i>											1					
<i>Klapperina unilabius</i>	1			5						1						
<i>Klapperina ovalis</i>	2	10	1	8		3		1								
<i>Palmatolepis transitans</i>											1?					
<i>Icriodus symmetricus</i>	8	2		46		7	11	1	25		124	23				
<i>Icriodus expansus</i>	2	1		15	2	1	1				5					
<i>Ozarkodina sp.</i>				1												
<i>Mehlina gradata</i>				1							1	2	1			
<i>Belodella sp.</i>		1	4	3			2	5		1	5	6	7			
<i>Playfordia sp.</i>										1						
total Pa elements (and Belodella)	146	48	24	264	23	44	88	9	139	5	4	231	94	3	8	
number of Pa elements/kg	146	48	24	264	23	44	88	9	139	5	4	231	94	3	8	
Pb, M and S elements	93	111	61	172	41	78	65	17	81	6	21	71	121	11	37	

Table 3. Composition and frequency of conodonts at Wietrzna W-IdW. Sample weight: S, below 0.5 kg, M, 0.5–1 kg, L, above 1 kg.

conodont zones		<i>Palmatolepis transitans</i>												<i>Palmatolepis punctata</i>								<i>Pa. hassi</i> s.l.										
ancyrodellid level		<i>Ancyrodella africana</i> – <i>A. pramosica</i>												<i>A.gigas</i> form 1				<i>A.gigas</i> form 2				<i>A.curvata</i>		<i>A.gigas</i> f.3								
sample weight		M	L	M	L	L	L	L	L	L	L	L	M	L	L	L	L	M	M	L	L	L	L	M	M	M	S					
taxa	sample number	3	9	10	11	15	21	22	25	27	35	37	40	41	42/1	42/2	43	45	46	47	49/1	49/2	50/1	50/2	51	53	54	55				
<i>Ancyrodella rugosa</i>	7	15	34	19	12	20	2	6	2	3	1																					
<i>Ancyrodella alata</i>	4	3	16	4	7	2		2	1	7	7	2		1																		
<i>Ancyrodella rotundiloba</i>	4	6	2		1	1					3		1																			
<i>Ancyrodella triangulata</i>	12	9	1																													
<i>Ancyrodella recta</i>			4							1		1																				
<i>Ancyrodella africana</i>	1?								2?		1	7	2		3	2	1															
<i>Ancyrodella pramosica</i>											2		1																			
<i>Ancyrodella gigas</i> form 1											5aff.		1aff.	2	3	2		1	2	4	1	3	1	1	1	1						
<i>Ancyrodella gigas</i> form 2																		1	1	2												
<i>Ancyrodella lobata</i>																								2	1							
<i>Ancyrodella curvata</i> early form																								1?	6	3	4					
<i>Ancyrodella gigas</i> form 3																											1					
<i>Ancyrodella</i> sp.	2	2	5	4	11	5	4			1	5		2	1	3					3				2	1	1						
<i>Polygnathus pennatus</i>	2	2	1	2						5		2																				
<i>Polygnathus dubius</i>	10	50	155	116	77	46	39	7	11	1	7	59	1	5	14	12	121	8	2	4	5	2	2	2								
<i>Polygnathus dengleri</i>	3	38	74	84	6	22	3			1		1																				
<i>Polygnathus aequalis</i>	2	11	38	21	4	5				15	1		2	2	2	13	2			4	13	3	4	1	6	14	11					
<i>Polygnathus pollocki</i>	1												3					1		2	1						1					
<i>Polygnathus webbi</i>	1		2			1				2		1	3				96	32	6	13		1	4	34	13	39						
<i>Polygnathus angustidiscus</i>	2	1		1	3	1	1			3		3	1			2	4	3	3	8	1	3		1	1	4	1					
<i>Polygnathus decorosus</i>	4	4	3	6					5	80	2	7	3	9	125	35			9	57	10	6	5	4	4		1					
<i>Polygnathus alatus</i>		3		2	1	4			1		2			3	13	7	1							1		2						
<i>Polygnathus lingulatus</i>									2?																							
<i>Polygnathus robustus</i>										1?			1	1	4																	
<i>Polygnathus foliatus</i>																	11	3	12	3aff.	1		2	2		1						
<i>Polygnathus uchtensis</i>																	4			5							2					
<i>Polygnathus brevilamiformis</i>																	12															
<i>Polygnathus timanicus</i>																	3															
<i>Polygnathus pacificus</i>																	6	10	3	3			1	7	2							
<i>Polygnathus lodinensis</i>																																
<i>Polygnathus</i> sp.										4	1	4	4	6	24		6	10	4	1	5	4	2	5	3	5	5					
<i>Palmatolepis transitans</i>												1					2	1	1	1												
<i>Palmatolepis punctata</i>																	1cf	1									1	1	1			
<i>Palmatolepis</i> sp. A																	2	1									1	4				
<i>Palmatolepis plana</i>																												4	1			
<i>Palmatolepis hassi</i> s.l.																												2	1			
<i>Palmatolepis</i> aff. <i>proversa</i>																												1				
<i>Palmatolepis</i> sp.																		1										1				
<i>Klapperina ovalis</i>	3	2	12	3	2						1		3		5	2	9	19	2	3	3			5			2					
<i>Klapperina unilabius</i>	3		8			1					1		5	2																		
<i>Mesotaxis falsiovalis</i>	1	10	20	18	18	22	18	2		1	5	8			6	2	2	8		5	2		1									
<i>Mesotaxis asymmetrica</i>										1	1	4	3		2	1																
<i>Mesotaxis bogoslovskyi</i>												1		2																		
<i>Mesotaxis costaliformis</i>												1cf		1																		
<i>Icriodus expansus</i>	6	7	37	3							11	2		1													1	3	8			
<i>Icriodus symmetricus</i>	1	19	31	67	5	20	8			16	61	25	1	9	16	3		2	3	1	1	1	1				1	3				
<i>Ag. aycrognathoides</i>											5	3		2							1						2	1	1			
<i>Mehlina gradata</i>						2		1																				2	1	1		
<i>Ozarkodina trepta</i>																													2	6	2	
<i>Ozarkodina nonaginta</i>																																
<i>Belodella</i> sp.	6		21	8	1	3	2	2		14	4	1	1	2	1	30	5			3	2	1	4		4	2						
<i>Playfordia</i> sp.			2	3		3				3	2					1																
total Pa elements (and Belodella)	32	154	396	427	185	146	146	20	27	3	83	261	57	7	56	43	93	297	71	158	92	46	163	38	28	17	27	53	61	80	219	34
number of Pa elements/kg	32	102	396	284	123	97	104	15	19	2	59	186	41	5	56	30	62	212	50	158	92	33	116	25	20	11	18	53	61	80	219	54
Pb, M and S elements	93	183	390	231	92	61	92	110	17	13	123	105	178	23	172	89	142	278	66	191	186	64	205	198	36	34	42	39	62	55	92	36

Table 4. Composition and frequency of conodonts at Kowala. Sample weight: S, below 0.5 kg, M, 0.5–1 kg, L, above 1 kg. Abbreviation: *A. afr.*—*A. pr.*, *Ancyrodella africana*—*A. pramosica*.

conodont zone	<i>Pa.transitans</i>		<i>Palmatolepis punctata</i>															
ancyrodellid level	<i>A. afr.</i> — <i>A. pr.</i>		<i>A. gigas</i> form 1								<i>Ancyrodella gigas</i> form 2							
sample weight	M	M	M	M	M	M	M	M	M	M	M	M	M	M	M	M	M	M
sample number taxa	C3	D1	D3	D5	D16	E1	E8C	E16	E24	E26	E29	F1	F2	F5	F7	F9	F10	
<i>Ancyrodella africana</i>	2	1	2			1												
<i>Ancyrodella rotundiloba</i>			1															
<i>Ancyrodella gigas</i> form 1			2	1	1	1						3		1				
<i>Ancyrodella gigas</i> form 2												1		1				
<i>Ancyrodella</i> sp.			2															
<i>Polygnathus dubius</i>	5	1	2	16	5	1			1					1				
<i>Polygnathus angustidiscus</i>				3								1	3	3	1	4		
<i>Polygnathus pollocki</i>				1	2	1			3	1	19					13	8	
<i>Polygnathus decorosus</i>				1	2		1				2							
<i>Polygnathus aequalis</i>					1		41	2	3									
<i>Polygnathus alatus</i>						1	1	17	1	27	2							
<i>Polygnathus pacificus</i>						1?		9	1	10	1	2	14	9	1			
<i>Polygnathus webbi</i>								32	7	15	14	2	24		2			
<i>Polygnathus uchensis</i>									1					3	20			
<i>Polygnathus brevilamiformis</i>											16	3	5	4	17	25		
<i>Polygnathus efimovae</i>											4							
<i>Polygnathus lingulatus</i>											1aff.							
<i>Polygnathus elegantulus</i>											6		1					
<i>Polygnathus gracilis</i>											5?							
<i>Polygnathus timanicus</i>												2		5				
<i>Polygnathus</i> sp.	4	2		3			8	3	16				9	13				
<i>Palmatolepis transitans</i>					2	1				9?								
<i>Palmatolepis punctata</i>									2	28	1	6	3	4	4			
<i>Palmatolepis</i> sp. A							2											
<i>Palmatolepis triquetra</i>											1aff.							
<i>Palmatolepis plana</i>													1?					
<i>Palmatolepis</i> sp.									35	2	4							
<i>Mesotaxis falsiovalis</i>							9				2	1						
<i>Klapperina unilabius</i>		2	5	1			2	1		1	18	3	14	3	15	3		
<i>Klapperina ovalis</i>							2	1		4	4	13	19	28	7			
<i>Icriodus symmetricus</i>		2	11				2	5	2	12	2	15	6	53	1			
<i>Icriodus expansus</i>			1				1		45	2			3					
<i>Ozarkodina postera</i>										1								
<i>Ozarkodina bidentatiformis</i>											2	6						
<i>Ozarkodina</i> sp.				1					2									
total Pa elements	5	3	13	45	10	13	2	5	129	20	12	401	40	68	85	169	89	
number of Pa elements/kg	5	3	13	45	10	13	2	5	129	20	12	401	40	68	85	169	89	
Pb, M and S elements	11	3	10	39	10	8	0	3	89	6	7	112	27	41	49	97	120	

Table 5. Composition and frequency of conodonts at Śluchowice. Sample weight: S, below 0.5 kg, M, 0.5–1 kg, L, above 1 kg. Abbreviation: A. afr.–A. pr., *Ancyrodella africana*–*A. pramosica*.

conodont zones	<i>Palmatolepis transitans</i>					<i>Palmatolepis punctata</i>															Pa. hassi s.l.										
ancyrodellid level	A.afr.–A.pr.					<i>Ancyrodella gigas</i> form 1															A.gigas form 2					A. curvata					
sample weight	S	M	M	S	S	M	M	M	S	S	S	S	S	S	S	S	S	S	S	S	S	M	M	M	M	M	M	M			
sample number taxa	13	14	15a	15b	16	17	19	23	24	25	26	27	28	29	34	36	37	41	43	47	49	52	56	59	68	78	83	89	94	97	
<i>Ancyrodella soluta</i>					1	2																									
<i>Ancyrodella rugosa</i>					1																										
<i>Ancyrodella rotundiloba</i>					1	1		1																							
<i>Ancyrodella pramosica</i>					54	20		1			2							1													
<i>Ancyrodella africana</i>					3	4		1	2	1								3	1cf.												
<i>Ancyrodella gigas</i> form 1					13	2		3	1	2	1	1		1		1	17			3			1		2	2	1				
<i>Ancyrodella gigas</i> form 2																							2		2	1	1				
<i>Ancyrodella curvata</i> early form																												2			
<i>Ancyrodella</i> sp.		1			7	9	1	2	3	1	2	1	1				4		4							3	1	1			
<i>Polygnathus pennatus</i>	1				3	1																									
<i>Polygnathus angustidiscus</i>	1	1				1			2	1	2		1				1	1	3	2											
<i>Polygnathus dubius</i>	3	4	1	28	10	1	3	17	11	26	5	4	1	3	13	11	49	11	6	1	10	7									
<i>Polygnathus decorosus</i>	1	4	3	9	59	24	5	44	7	2	38	2	1	1	5	7	19	20	18	92	12	6	17			8	9				
<i>Polygnathus</i> aff. <i>decorosus</i>					3	4			2	1	4	1			1	5	5	14	2												
<i>Polygnathus alatus</i>	1				1	4	4		5		2	2	2		1	4	1	9	3	2						4					
<i>Polygnathus aequalis</i>					21	6		35	13	5	46	5	3	2	4	7	46	55	16	9	5	4	116								
<i>Polygnathus foliatus</i>						1		1							3		3														
<i>Polygnathus elegantulus</i>					2										1	3?										2	1				
<i>Polygnathus rudkinensis</i>					2aff.																					2	7	3			
<i>Polygnathus webbi</i>		2						2		1			1	1		4	20	23	19	2	1	68	9	4	34	22	6	2			
<i>Polygnathus lingulatus</i>														1aff.												3	1				
<i>Polygnathus pacificus</i>																4	3									5	7				
<i>Polygnathus uchtensis</i>																										14					
<i>Polygnathus timanicus</i>																										4	2	1			
<i>Polygnathus brevilamiformis</i>																										13	2	5	7	2	
<i>Polygnathus</i> sp.	2	2		3	11	4	9	23	10	7	15		4	4	4	3		5	14		5	3	22	5	3	5		4	15		
<i>Palmatolepis transitans</i>		1		1	1				1	1	3							2	1									1			
<i>Palmatolepis punctata</i>																1										1	2	1	3		
<i>Palmatolepis bohemica</i>																												2			
<i>Palmatolepis plana</i>																													1		
<i>Mesotaxis falsiovalis</i>		1	1	3	13		2	2	1	20	2	1	1	3	3		6	3	1	4	7								1		
<i>Mesotaxis asymmetrica</i>			2	39	10		1	4	8	2	3	9	1	4		9	1	1	1	4											
<i>Mesotaxis costalliformis</i>	2		65	4												5	4	4	4	2		1	11	2	6	39	7	6			
<i>Klapperina ovalis</i>	1		1?	3		4	6	7	1	3		4			5	4	4	4	2		1	11	2	6	39	7	6				
<i>Klapperina unilabius</i>		1							1				2	2	3	6	1					2	2	3	2	1					
<i>Icriodus symmetricus</i>	1		1	2	41	51	15	2	1	1	2	2	1		1		4	5	2	1	3	2	15		5	2		2			
<i>Icriodus expansus</i>								1		1						2	4	3	1												
<i>Icriodus</i> sp.														2																	
<i>Ancyrognathus</i> sp. A						5																									
<i>Ag. ancyrognathoides</i>																										1	1	1			
<i>Mehlina gradata</i>						1	1																			3					
<i>Ozarkodina</i> sp.							1											3													
<i>Playfordia</i> sp.	1					1	6																								
<i>Belodella</i> sp.	1					1	5	1									1		1												
total Pa elements (and Belodella)	4	9	16	10	301	218	55	34	131	75	21	171	19	32	11	25	83	98	220	113	137	31	31	300	36	17	120	49	50	56	
number of Pa elements/kg	5	9	16	12	421	218	55	34	163	93	30	244	27	45	15	38	118	140	314	141	162	45	45	300	36	17	120	49	50	56	
Pb, S and M elements	12	28	26	35	256	161	36	31	76	76	45	104	18	13	16	48	44	192	161	93	97	48	15	109	28	9	63	40	74	69	

Table 6. Composition and frequency of conodonts at Mogilki. Sample weight: S, below 0.5 kg, M, 0.5–1 kg, L, above 1 kg. Abbreviation: A. afr.—A. pr., *Ancyrodella africana*—*A. pramosica*.

conodont zones	<i>Pa. transitans</i>						<i>Palmatolepis punctata</i>										<i>Pa. hassi</i> s.l.						
ancyrodellid level	A. afr.—A. pr.						A. <i>gigas</i> form 1					A. <i>gigas</i> form 2					A. <i>curvata</i>						
sample weight	M	L	M	M	L	M	L	M	M	M	M	M	M	M	S	M	M	M	M	S	M	S	
taxa	21	29	33	38	40	42	44	45	52	57	61	66	70	74	93	104	117	119	128	133	139	147	
<i>Ancyrodella rotundiloba</i>	1	4	2																			154	
<i>Ancyrodella rugosa</i>	3																						
<i>Ancyrodella alata</i>	24	18																					
<i>Ancyrodella triangulata</i>	6	3																					
<i>Ancyrodella recta</i>	8	1																					
<i>Ancyrodella pramosica</i>	3																						
<i>Ancyrodella africana</i>					3		5		2														
<i>Ancyrodella gigas</i> form 1							1			1	1	1		1									
<i>Ancyrodella gigas</i> form 2												1?		1									
<i>Ancyrodella lobata</i>															1								
<i>Ancyrodella curvata</i> early form																		2	1	2	1		
<i>Ancyrodella</i> sp.	4	4		1		1	1	5	2		1										1		
<i>Polygnathus pennatus</i>	4?									1													
<i>Polygnathus dubius</i>	102	16	19	3	6	20	5	92	7	14	2												
<i>Polygnathus webbi</i>	1					1		2			36	2	8		2	2	1	1	3	1			
<i>Polygnathus aequalis</i>	34	12	2			10	10	20	40	68			1		1	2				4	7		
<i>Polygnathus decorosus</i>	7	7			2	23	4	14	2	12	22		2	3			1						
<i>Polygnathus alatus</i>	1						4			25	2												
<i>Polygnathus dengleri</i>	4	3	2																				
<i>Polygnathus angustidiscus</i>	1	2								2													
<i>Polygnathus pollocki</i>					19		3	9	2	2			7										
<i>Polygnathus aff. decorosus</i>													4										
<i>Polygnathus elegantulus</i>														5									
<i>Polygnathus pacificus</i>														5									
<i>Polygnathus brevilamiformis</i>														5									
<i>Polygnathus rudkinensis</i>											3												
<i>Polygnathus uchtensis</i>											21	2			4		1	4					
<i>Polygnathus</i> sp.	9	8			18	7	8	17	8	11	2	1		2		2	2	9		4	2		
<i>Palmatolepis transitans</i>					2	1	11	6	2	5													
<i>Palmatolepis punctata</i>										5	1		1	1	3	2	13	1		1			
<i>Palmatolepis bohemica</i>																39	3	4					
<i>Palmatolepis plana</i>																1							
<i>Palmatolepis hassi</i> s.l.																1	3	1					
<i>Palmatolepis</i> sp. A																							
<i>Mesotaxis falsiovalis</i>	8	1		14	7	4	8	9	23	21		1	3										
<i>Mesotaxis asymmetrica</i>	39	46			4		3	60	3	2	4												
<i>Mesotaxis bogoslovskyi</i>							2																
<i>Mesotaxis costalliformis</i>							1																
<i>Klapperina unilabius</i>	3			1		3	17	7	31			4											
<i>Klapperina ovalis</i>	4			1	2	2	12	13	15	29	8	16	4										
<i>Ag. ancyrognathoides</i>										1		1											
<i>Icriodus symmetricus</i>	31	38	16	1		2	6	22		4	110	2					2			3	3		
<i>Icriodus expansus</i>							1	8									4			4	3		
<i>Ozarkodina postera</i>															2								
<i>Ozarkodina trepta</i>																4							
<i>Mehlina gradata</i>		1														1							
<i>Playfordia</i> sp.	1	1	1																				
total Pa elements	282	172	45	5	27	100	45	271	103	138	414	21	29	18	4	11	2	11	80	16	8	19	15
number of Pa elements/kg	282	132	45	5	22	100	45	271	103	138	414	21	29	18	4	15	2	11	80	16	11	19	15
Pb, M and S elements	91	74	50	8	38	148	72	354	132	295	269	33	46	37	8	37	5	14	64	6	14	22	19

Table 7. Composition and frequency of conodonts at Dębnik. Sample weight: S, below 0.5 kg, M, 0.5–1 kg, L, above 1 kg. Abbreviation: A. afr.–A. pr., *Anceroedella africana*–*A. pramosica*.

conodont zones		?		Pa. transitans						Palmatolepis punctata													
ancyrodellid level		?		A.afr. A.pr.?				A. afr.–A.pr.				Ancyrodella gigas form 1						A. gigas form 2					
sample weight		M	M	L	M	M	M	M	M	M	M	M	M	M	M	M	M	M	M	M	M	M	
taxa	sample number	46	48	49	51B	54	58	59	60	61	62A	62B	63	73	77	80	82	89	92	93	94	96	100
<i>Ancyrodella alata</i> (early form)	1																					106	
<i>Ancyrodella rugosa</i>			1																				
<i>Ancyrodella pramosica</i>				1	1?	1	2	16	9	41													
<i>Ancyrodella africana</i>					6		1	1	4	3	4												
<i>A. africana</i> → <i>A. gigas</i>								1	1		2												
<i>Ancyrodella gigas</i> form 1								1	9	17		2	2					1	2	5			
<i>Ancyrodella triangulata</i>									4	6	1												
<i>Ancyrodella recta</i>										4													
<i>Ancyrodella</i> sp.					1	1		1	4		1												
<i>Polygnathus pennatus</i>	6	2	7	8		4		4	3		1												
<i>Polygnathus dubius</i>	7	15	50	2	11		4	9	41	10	3	3	2		4		5	1	2	5			
<i>Polygnathus angustidiscus</i>	6	2				1	2	4	3	2			2				1	1	3				
<i>Polygnathus decorosus</i>	15	1	5	3	2	7	19	9	9	7	2	1				1	14				1		
<i>Polygnathus aequalis</i>	4	6	15				1	2		5					14	4	67	2	13	59	40		
<i>Polygnathus robustus</i>							2	6		4					1			1	3				
<i>Polygnathus webbi</i>			2					4						1	1	2	53	1	1	36	3	31	
<i>Polygnathus timanicus</i>								2											2		2		
<i>Polygnathus alatus</i>					3										1	1	17	1	9				
<i>Polygnathus pollocki</i>								3								2?	6	18	2				
<i>Polygnathus foliatus</i>									7														
<i>Polygnathus brevilamiformis</i>																1		2		5			
<i>Polygnathus uchtensis</i>																	2	86		21			
<i>Polygnathus lodinensis</i>																	1	5		25			
<i>Polygnathus elegantulus</i>																	3						
<i>Polygnathus efimovae</i>																		1					
<i>Polygnathus pacificus</i>								2										9		8			
<i>Polygnathus</i> aff. <i>rudkinensis</i>	5		10		6	1	2			8		1		3	2	14	2	8	16	1	15		
<i>Polygnathus</i> sp.	5							4	3	2		1				10	7	2					
<i>Palmatolepis transitans</i>												1											
<i>P. transitans</i> → <i>P. punctata</i>																							
<i>Palmatolepis punctata</i>																	9	2	13	18	5	2	
<i>Palmatolepis bohemica</i>																1			1aff				
<i>Palmatolepis hassi</i> s.l.																					1?		
<i>Palmatolepis</i> sp. A																1	1	1	1	1	2		
<i>Klapperina ovalis</i>	2								5						1		4	9	16	2	7		
<i>Mesotaxis falsiovalis</i>	1		1					2	9					2			2	1	6		9		
<i>Klapperina unilabius</i>							1				5											9	
<i>Mesotaxis asymmetrica</i>				1		10		3	17	69	7	1	6	2	4	8	1	1	4				
<i>Mesotaxis costallifromis</i>									7	6													
<i>Mesotaxis bogoslovskyi</i>									3	10													
<i>Icriodus symmetricus</i>	2	1	64	191	6	83		78	52	18	2	3	3	6	4	8	3	19	31	46	2		
<i>Icriodus expansus</i>	18	6	101	42	4	6		6	7							1			10				
<i>Mehlina gradata</i>									1		1												
<i>Ozarkodina postera</i>																	1				2		
<i>Ozarkodina</i> sp.											1							1					
<i>Playfordia</i> sp.			5					2	1														
<i>Belodella</i> sp.	3		9		1		3														3		
total Pa elements (and Belodella)	66	14	210	322	14	138	5	123	172	203	106	35	16	17	9	41	18	217	18	111	346	18	
number of Pa elements/kg	66	14	150	322	14	138	5	123	172	203	106	25	16	17	9	41	18	155	18	111	247	18	
Pb, M and S elements	108	13	96	94	9	46	14	79	241	157	162	25	17	5	6	36	26	152	8	128	178	8	